San Jose State University
SJSU ScholarWorks

Master's Theses | Master's Theses and Graduate Research

Spring 2014

Development of a Spatial Filtering Apparatus

Nicolle Wilson
San Jose State University

Follow this and additional works at: https://scholarworks.sjsu.edu/etd_theses

Recommended Citation
Wilson, Nicolle, "Development of a Spatial Filtering Apparatus" (2014). *Master's Theses*. 4444.
DOI: https://doi.org/10.31979/etd.9kqs-gz2j
https://scholarworks.sjsu.edu/etd_theses/4444

This Thesis is brought to you for free and open access by the Master's Theses and Graduate Research at SJSU ScholarWorks. It has been accepted for inclusion in Master's Theses by an authorized administrator of SJSU ScholarWorks. For more information, please contact scholarworks@sjsu.edu.

DEVELOPMENT OF A SPATIAL FILTERING APPARATUS

A Thesis

Presented to

The Faculty of the Department of Physics and Astronomy

San José State University

In Partial Fulfillment

of the Requirements for the Degree

Master of Science

by

Nicolle Wilson

May 2014

© 2014

Nicolle Wilson

ALL RIGHTS RESERVED

The Designated Thesis Committee Approves the Thesis Titled

DEVELOPMENT OF A SPATIAL FILTERING APPARATUS

by

Nicolle Wilson

APPROVED FOR THE DEPARTMENT OF PHYSICS AND ASTRONOMY

SAN JOSÉ STATE UNIVERSITY

May 2014

Dr. Peter Beyersdorf	Department of Physics and Astronomy
Dr. Kenneth Wharton	Department of Physics and Astronomy
Dr. Ramendra Bahuguna	Department of Physics and Astronomy

ABSTRACT

DEVELOPMENT OF A SPATIAL FILTERING APPARATUS

by Nicolle Wilson

This thesis contains a discussion of the theoretical background for Fourier spatial filtering and a description of the design and construction of a portable in-class spatial filtering apparatus. A portable, in-class spatial filtering demonstration apparatus was designed and built. This apparatus uses liquid crystal display (LCD) panels from two projectors as the object and filter masks. The blue LCD panel from the first projector serves as the object mask, and the red panel from the second projector serves as the filter mask. The panels were extracted from their projectors and mounted onto aluminum blocks which are held in place by optical component mounts. Images are written to the LCD panels via custom open source software developed for this apparatus which writes independent monochromatic images to the video signal. The software has two monochromatic image windows, basic image manipulation tools, and two video feed input display windows. Two complementary metal-oxide semiconductor (CMOS) sensors are positioned to record the reconstructed image of the object mask and the diffraction pattern created by the object mask. The object and filter mask can be digitally changed and the effects on the filtered image and diffraction pattern can be observed in real-time. The entire apparatus is assembled onto a rolling cart which allows it to be easily taken into classrooms.

DEDICATION

To my son, Justin, and husband, Jeff.

ACKNOWLEDGEMENTS

I would like to thank everyone for helping me through my journey.

Special thanks to my husband, Jeff, and son, Justin for their patience, support, and encouragement. Special thanks to my advisor, Dr. Peter Beyersdorf, for his help, expertises, and providing me with a thesis project. Special thanks to Troy Fisher for writing custom open source software which is used in this project. Special thanks to Thao Le for all of his metal work. Special thanks to all of my professors at San Jose State University. Special thanks to my co-workers who have helped me with practical issues along the way. Thank you to my family, friends, and co-workers for their patience while I complete my degree. And thank you to Schafer Corporation for providing financial support for my degree.

TABLE OF CONTENTS

CHAPTER

LIST OF FIGURES

Figure

CHAPTER 1

INTRODUCTION

1.1 Importance of Fourier Optics

Fourier optics is the underlying principle studied in most graduate level optics courses. It explores the transmission of an electric field through an optical system. It considers the transmission of spatial frequencies and the phase delays acquired by the electric field while traveling through the system. As opposed to ray optics, which only studies the effects of reflection and refraction, Fourier optics studies the effects of diffraction, the bending of light around obstacles. When light diffracts through an aperture, it creates a diffraction pattern. The characteristics of the diffraction pattern depend on the physical characteristics of the diffracting object and the light and the point at which the diffraction pattern is viewed.

Fourier Optics is extensively used in many fields. A few of them are image analysis, material fabrication, material characterization, astronomy, high-precisions optics, optical microscopy, and spectral analysis. This thesis will focus on diffracting objects, their characteristic diffraction patterns, and experimental techniques which can be used to analyze those patterns and the diffracting objects.

1.2 Classic Spatial Filtering

Under certain circumstances, the diffraction pattern created by the aperture is a Fourier transform of the aperture itself. Therefore, a diffraction pattern contains spatial frequency information about the structure of the diffracting aperture.

Spatial filtering is the process of blocking certain areas of a diffraction pattern to allow only select spatial frequencies to pass. This will effect any reconstructed image of the diffracting aperture.

A two-lens imaging system can be constructed where an image of an object mask can be spatially filtered to allow only certain features of the object to be present in the final image. A common geometry used for such purposes is known as a 4F system (see Figure 1.1). An object mask is illuminated with spatially coherent light. A lens with focal length f is placed one focal length away from a diffracting object. A second lens is placed a distance two focal lengths away from the first lens. The image of the object mask is created one focal length away from the second lens. Between the two lenses is the diffraction pattern created by the object mask. At this plane, a filter mask can be placed which will block certain areas of the object mask. Each point in the diffraction pattern strongly corresponds to a feature in the object mask. By blocking this area in the diffraction pattern, the corresponding feature will not appear in the image [1].

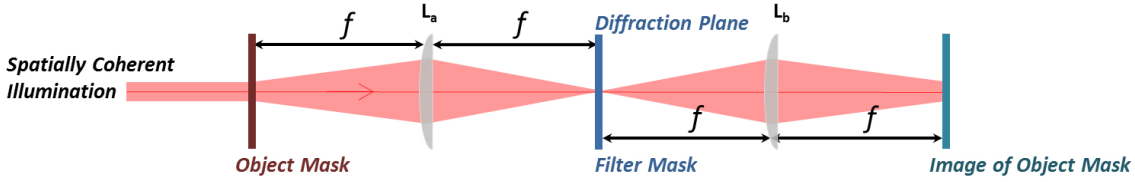

Figure 1.1: Diagram of 4F system.

Spatial filtering has several applications. By using a spatial filter which corresponds to the diffraction pattern of a specific shape, that shape can be detected (or not detected) in the object mask. Images which are highly pixelated (such as newsprint images) can be passed through a low pass filter to create a smoother appearing image. Images can be passed through a high pass filter to

enhance the appearance of fine-detail or edges. Diffraction patterns of objects can be examined to detect any deviation from a "normal" appearance of a diffraction pattern of an object. Such a comparison between diffraction patterns is typically easier for a computer to handle, as opposed to a comparison of objects themselves.

The object and filter mask in a typical 4F experiment are often static features (either a printed image on a transparency or a physical filter mask). Printed transparencies can have low contrast values, which allow light from the entire object mask to leak through and create incomplete spatial filtering. Because the images are printed, they cannot be scaled in real time. Also, if one wishes to change either the object or the filter mask, one must manually change the transparencies and potentially have to realign the masks to ensure proper filtering and imaging.

1.3 Experiment and Improvements

A system in which the object and filter mask have a high contrast value and are dynamically changed via computer software would be an improvement over the standard construction. It would also be desirable to view both the reconstructed image of the object and the diffraction pattern created by the object in real time.

This paper contains a discussion of the theoretical background for Fourier spatial filtering and a description of the design and construction of a portable in-class spatial filtering apparatus.

CHAPTER 2

FOURIER OPTICS

A plane monochromatic light wave traveling in free space has both an electric and magnetic field, which oscillate sinusoidally. These fields oscillate perpendicularly to each other, and both oscillate perpendicular to the direction of propagation. For a plane wave propagating in the z-direction, the equations which describe these fields can be expressed as:

$$\begin{aligned} \vec{E}(z,t) &= \mathrm{Re}\left\{\vec{E}_0 e^{-i(kz-\omega t)}\right\} \qquad \text{Electric Field} \\ \vec{H}(z,t) &= \mathrm{Re}\left\{\vec{H}_0 e^{-i(kz-\omega t)}\right\} \qquad \text{Magnetic Field} \end{aligned} \tag{2.1}$$

where $\vec{E}_0$ and $\vec{H}_0$ are the amplitude vectors of their respective waves, k is the wavenumber (where $k = \frac{2\pi}{\lambda}$ and λ is the wavelength), ω is the angular frequency, and t is time [2].

2.1 Polarization

As the wave propagates in the z-direction, the electric field vector traces out a shape in the x-y plane. This shape describes the polarization of the light. The electric field from Equation 2.1 has components which can written as

$$\begin{aligned} E_x &= \mathrm{Re}\left\{E_{x0} e^{-i(kz-\omega t)}\right\} \\ E_y &= \mathrm{Re}\left\{E_{y0} e^{-i(kz-\omega t-\phi)}\right\} \end{aligned} \tag{2.2}$$

where ϕ is the relative phase delay between the x and y components. Light can be linearly polarized in which ϕ=0 and the shape in the x-y plane is a line, circularly

polarized in which $\phi = \pm\frac{\pi}{2}$, $E_{x0} = E_{y0}$, and the shape in the x-y plane is a circle, or elliptically polarized (the most general case) in which $0 \leq \phi \leq 2\pi$ and the shape in the x-y plane is an ellipse [3]. When a light source has no specific polarization direction, or is chaotically and rapidly switching between different polarization directions, it is described as "unpolarized." Many light sources produce unpolarized light (i.e., the sun, incandescent light bulbs, and some lasers).

2.2 Interference

Light detectors measure the irradiance of the electric field. The irradiance is proportional to E^2. When multiple waves overlap in space, the electric fields combine using the principle of superposition. The resulting irradiance, however, is not a simple addition of the irradiance of each contributing wave function. The calculation of the irradiance of two overlapping waves is discussed below.

Assume two monochromatic waves with frequency f and complex amplitudes, $\widetilde{E}_1$ and $\widetilde{E}_2$, combine in space. The resulting wave has a complex amplitude

$$\widetilde{E}_{total} = \widetilde{E}_1 + \widetilde{E}_2. \tag{2.3}$$

The irradiance, I, of the resulting wave is proportional to the absolute value squared of the resulting electric field,

$$I \propto |\widetilde{E}_{total}|^2. \tag{2.4}$$

Substituting Equation 2.3 into 2.4 gives

$$\begin{aligned} I &\propto |\widetilde{E}_1 + \widetilde{E}_2|^2 \\ &\propto |\widetilde{E}_1|^2 + |\widetilde{E}_2|^2 + E_1^* E_2 + E_1 E_2^*. \end{aligned} \tag{2.5}$$

If we substitute

$$E_1 = \sqrt{I_1}e^{(-i\phi_1)} \quad \text{and} \quad E_2 = \sqrt{I_2}e^{(-i\phi_2)} \tag{2.6}$$

(where ϕ_1 and ϕ_2 are the phases of each wave) into equation 2.5 and let $\phi = \phi_2 - \phi_1$ we get

$$I = I_1 + I_2 + 2\sqrt{I_1 I_2}\cos(\phi). \tag{2.7}$$

The ϕ term is the phase delay between two waves (as shown in Figure 2.1). Equation 2.7 is the interference term. When $\phi = 0$ or 2π, the waves are in phase, and their electric field amplitudes add completely. When $\phi = \pi$, the waves are out of phase, resulting in an electric field with zero amplitude. In general, when $|E_{total}|^2$ is larger than $|E_1|^2$ or $|E_2|^2$, it is known as constructive interference. When $|E_{total}|^2$ is smaller than $|E_1|^2$ or $|E_2|^2$, it is known as destructive interference. This is important when considering diffraction patterns, as will be discussed in the following section.

2.3 Diffraction

To predict the path of propagating light, ray optics can be used. In ray optics only the effects of reflection and refraction are considered. However, when light passes through an aperture, it spreads out. This results in light being present in places not accounted for by reflection or refraction and is referred to as diffraction.

Diffraction is typically discussed in two regions. Near the diffracting object is the Fresnel region (the near-field). Far from the diffracting object is the Fraunhofer region (the far-field). In the Fraunhofer region, the diffraction pattern is proportional to the absolute value squared of the Fourier transform of the aperture function, as will be shown below.

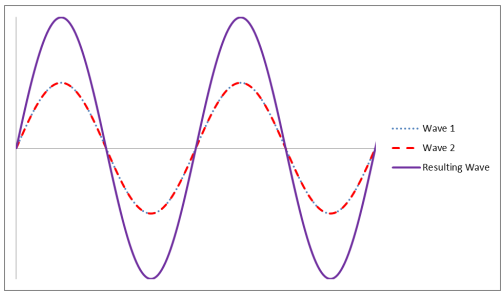

(a) $\phi = 0$ phase delay (in phase)

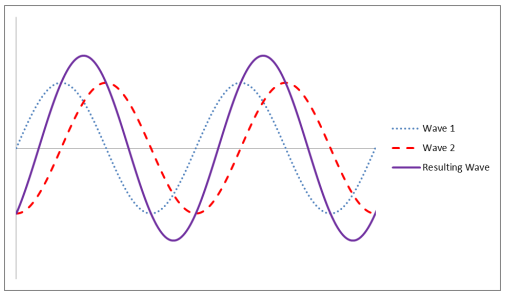

(b) $\phi = \frac{\pi}{2}$ phase delay

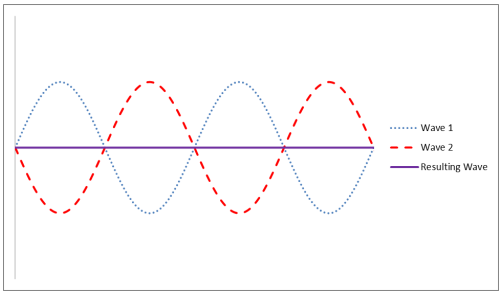

(c) $\phi = \pi$ phase delay (out of phase)

Figure 2.1: Diagrams of electric fields from two waves with the same frequency and amplitude occupying the same space combining to form a resulting wave. Sub-figures (a)-(c) show various phase delays of ϕ.

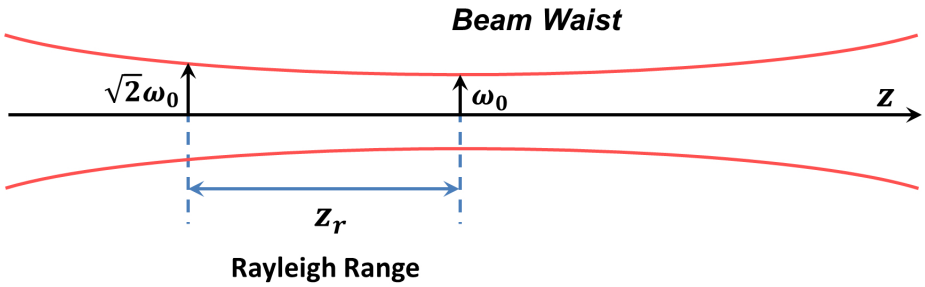

Figure 2.2: Diagram of a Gaussian beam propagating in the z-direction with a waist of ω_0 and a Rayleigh Range of z_r.

For a Gaussian beam (such as the output of the laser used in our apparatus) propagating in the z-direction, the beam waist is located where the beam radius has the smallest value, ω_0. When the cross sectional area is twice as large as it is at the beam waist, the beam radius has a value of $\sqrt{2}\omega_0$. The distance between the plane of the waist and the plane at which the cross sectional area is doubled, z_r, is the Rayleigh range (see Figure 2.2). The Rayleigh range is defined by

$$z_r = \frac{\pi\omega_0^2}{\lambda}. \tag{2.8}$$

The Fraunhofer region for a Gaussian beam is the range where $z >> z_r$. For a light source with wavelength $\lambda = 633$ nm and a waist $\omega_0 = 5.1$ cm, the Rayleigh range is 13 km. A lens can be used to reduce this distance and bring the diffraction pattern closer to the diffracting aperture. The plane in which this pattern can be clearly seen is known as the Fourier plane. If the illumination is a point source, the Fourier plane is colocated with the image of the source created by the lens. If the illumination is a collimated beam of light, the Fourier plane is located at a distance equal to the focal length of the lens [1] [4].

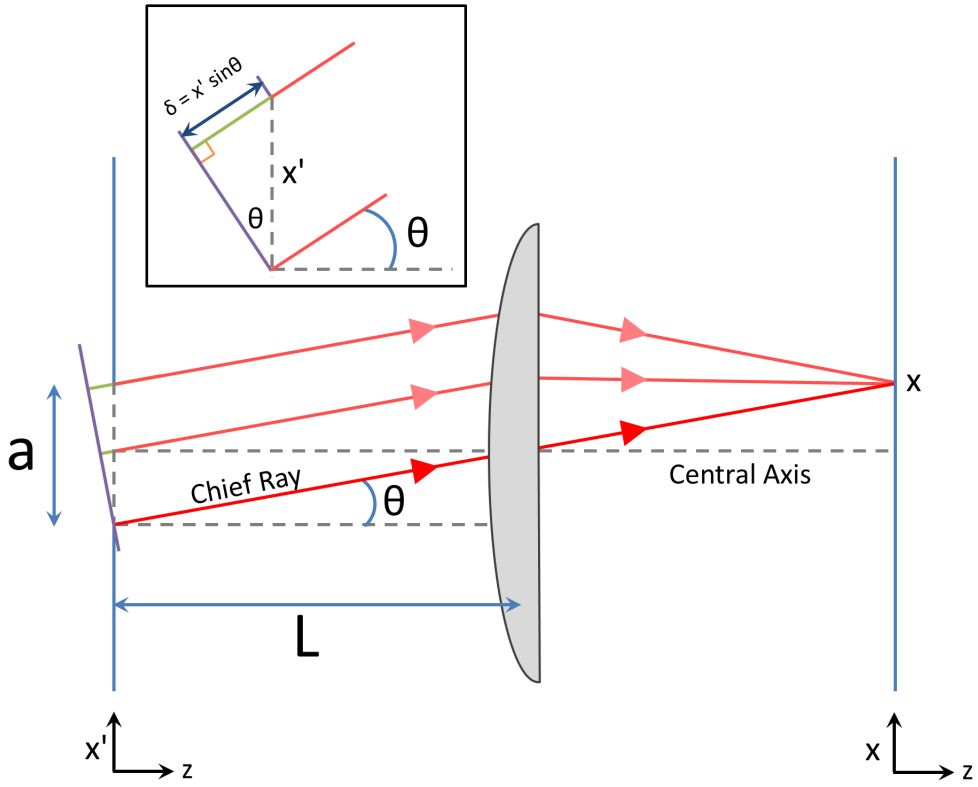

Figure 2.3: Diagram of Huygens principle showing wavefronts from several points along the aperture being focused to point x by a lens with focal length f.

Consider collimated light passing through a single rectangular aperture of width a and a lens placed a distance, L, away, with a focal point of x (see Figure 2.3). Huygen's principle states that each point on a wave front acts as a secondary source. To find the electric field at a focal point, x, the contribution from each point of the wavefront in the aperture must be considered. In general, for a point, x', in the aperture, the contribution to the field at point x is

$$E(x) = \left(\frac{L}{\cos\theta}\right)^{-1} \operatorname{Re}\{\vec{E}(x')e^{i(\omega t+\phi(x'))}\} \tag{2.9}$$

where $\left(\frac{L}{\cos\theta}\right)^{-1}$ is the attenuation of the E-field traveling from the aperture to the lens, and ϕ is the phase shift obtained from traveling from the aperture to the focal point, x. Using the small angle approximation of $\cos\theta \approx 1$, Equation 2.9 becomes

$$E(x) = \frac{1}{L} \operatorname{Re}\{\vec{E}(x')e^{i(\omega t+\phi(x'))}\}. \tag{2.10}$$

The chief ray is the ray which extends from the aperture through the center of lens without deviation to the focal point x [3]. The contribution to the electric field at point x from the chief ray is

$$E(x)_{x'} = \frac{1}{L} \operatorname{Re}\{\vec{E}(x')e^{i(\omega t+\phi_0)}\} \tag{2.11}$$

where ϕ_0 is the phase shift acquired by the chief ray.

Rays emitted from elsewhere in the aperture experience a different path length than the chief ray, and thus acquire a different phase shift. The electric field contribution to a point in the focal plane located at x by these rays can be defined as

$$E(x) = \frac{1}{L}E(x')e^{i(\omega t+(\phi_0-\Delta\phi(x')))} \tag{2.12}$$

where ϕ_0 is the phase shift acquired by the chief ray and $\Delta\phi(x')$ is the phase shift acquired by traveling a path length difference of $\delta(x')$. Figure 2.3 shows a plane

normal to the chief ray. The path length difference, $\delta(x')$, experienced by the other rays can be defined as the distance from the aperture to the normal line and can be expressed as

$$\delta(x') = x' \sin\theta. \tag{2.13}$$

Figure 2.4 shows k-vectors in the system. From this it can be shown that $k_{x'} = k_0 \sin\theta$ which can be substituted into Equation 2.13 to give

$$\delta(x') = x'\left(\frac{k_{x'}}{k_0}\right). \tag{2.14}$$

The phase shift, $\Delta\phi(x')$, associated with the path length difference of $\delta(x')$ is

$$\Delta\phi(x') = \frac{2\pi}{\lambda}\delta(x'). \tag{2.15}$$

Substituting Equation 2.14 and $k_0 = \frac{2\pi}{\lambda}$, we get

$$\Delta\phi(x') = k_{x'}x'. \tag{2.16}$$

The electric field at focal point x can be calculated by adding the contributions from all the points in the aperture

$$E(x) = \frac{1}{L}\int_{-\infty}^{\infty} E(x')e^{i(\omega t+(\phi_0-\Delta\phi(x')))}dx' \tag{2.17}$$

rearranging and substituting Equations 2.11 and 2.16 we get

$$E(x) = \frac{1}{L}\int_{-\infty}^{\infty} E(x')e^{-ik_{x'}x'}dx'. \tag{2.18}$$

Setting aside the $\frac{1}{L}$ factor a moment,

$$E(x) \propto \int_{-\infty}^{\infty} E(x')e^{-ik_{x'}x'}dx' \tag{2.19}$$

where the integral is the Fourier transform of $E(x')$ (see Section 2.7). This implies that the electric field distribution at the diffraction plane is proportional to the

Fourier transform of the electric field distribution at the aperture. This derivation is true of any arbitrary aperture field provided the illumination is spatially coherent.

Now consider the intensity pattern of a single slit aperture viewed on a screen placed a distance, D, away with no lens (see Figure 2.5). Recall that the intensity of light is to $|E|^2$. In the Fraunhofer region, the intensity pattern as a function of θ is

$$I(\theta) = I_0 \left(\frac{\sin \beta(\theta)}{\beta(\theta)} \right)^2 \tag{2.20}$$

with

$$\beta(\theta) = \frac{\pi a}{\lambda} \sin \theta. \tag{2.21}$$

Equation 2.20 is a sinc^2 function with a central maxima and a series of alternating bright and dark regions (fringes). This is the Fourier transform of the single slit step function [5]. The angular position, θ_m, of the m^{th} dark fringe, measured relative to the central peak, obeys the formula

$$a \sin \theta_m = m\lambda. \tag{2.22}$$

A dark fringe is a result of destructive interference from the wavefronts in the aperture function. Using the small angle approximation we can assume $\sin\theta \approx \tan\theta$ and set $\sin\theta_m \approx \frac{x}{D}$. Equation 2.22 can then be rewritten as

$$x_m \approx \frac{m\lambda D}{a} \tag{2.23}$$

where x_m is the distance from the center of the screen to the m^{th} dark fringe. This pattern can be mapped onto the focal plane of a lens by using the formula

$$\theta = \frac{x}{f}. \tag{2.24}$$

The light passing through the single slit is now spatially coherent in the far field.

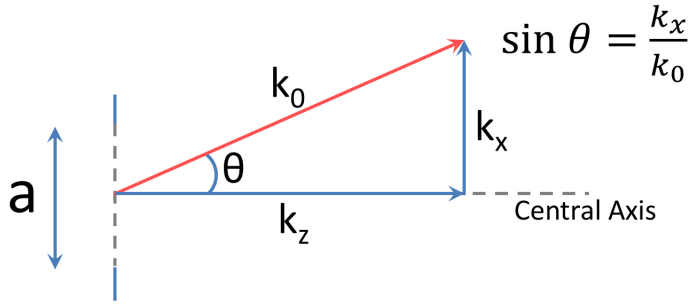

Figure 2.4: Diagram of k-vectors in an optical system.

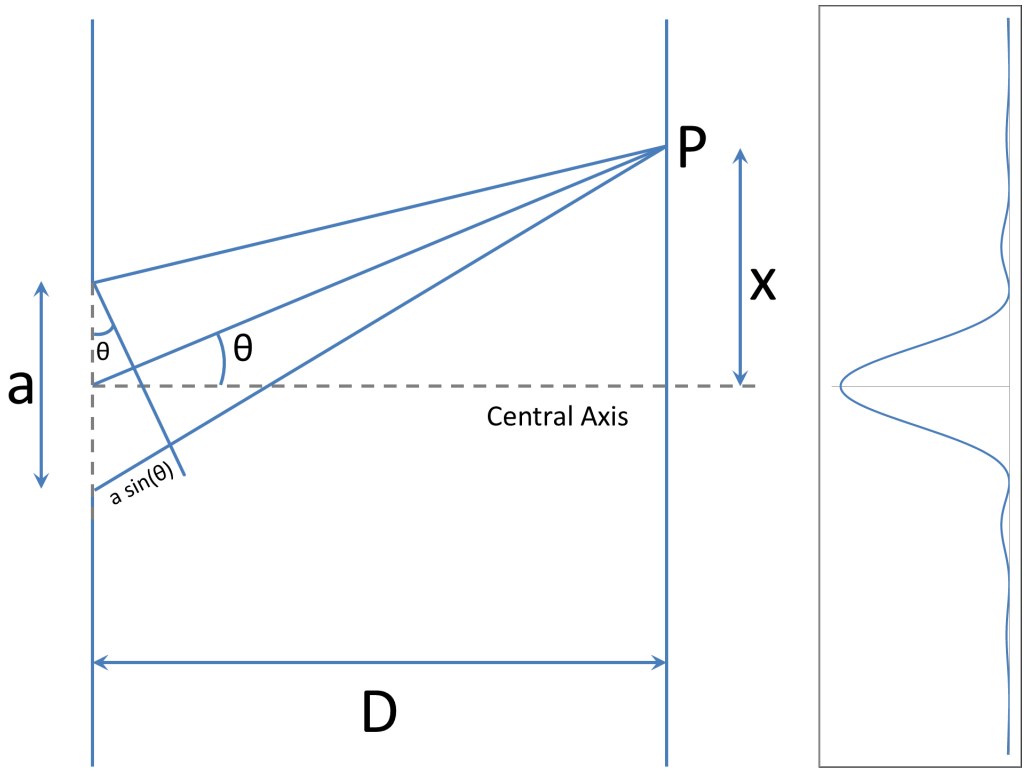

Figure 2.5: Diagram of single slit experiment with intensity profile.

Now consider placing two slits, each of width a, after the single slit. Assume the two slits are equidistant from the first slit. The two slits are separated by a distance d (see Figure 2.6). The interference pattern as a result of the path length difference between the two slits is

$$I(\theta) = I_{\max} \cos^2\left(\frac{\pi d \sin\theta}{\lambda}\right). \tag{2.25}$$

When the path length difference of the light passing through the two slits is equal to an integer value of the wavelength $(m\lambda)$, the waves constructively interfere and a bright fringe is produced. When the path length difference is equal to $(m + \frac{1}{2})\lambda$ the waves destructively interfere and a dark fringe is produced. The angular position, θ_m, of the m^{th} bright fringe, as measured relative to the central bright fringe, can be found by using the following formula

$$m\lambda = d \sin\theta_m. \tag{2.26}$$

Using the small angle approximation of $\sin\theta \approx \tan\theta$ and setting $\sin\theta_m \approx \frac{x}{D}$, Equation 2.26 can be rewritten as

$$x_m \approx \frac{m\lambda D}{d} \tag{2.27}$$

where x_m is the displacement from the center of screen to the location of the bright fringe.

The intensity pattern visible on the screen placed a distance, D, away, is a result of the interference pattern of the light from the two slits with an envelope of a single slit diffraction pattern,

$$I(\theta) = I_0 \left(\frac{\sin\beta(\theta)}{\beta(\theta)}\right)^2 \cos^2\left(\frac{\pi d \sin\theta}{\lambda}\right) \tag{2.28}$$

where

$$\beta(\theta) = \frac{\pi a}{\lambda} \sin\theta. \tag{2.29}$$

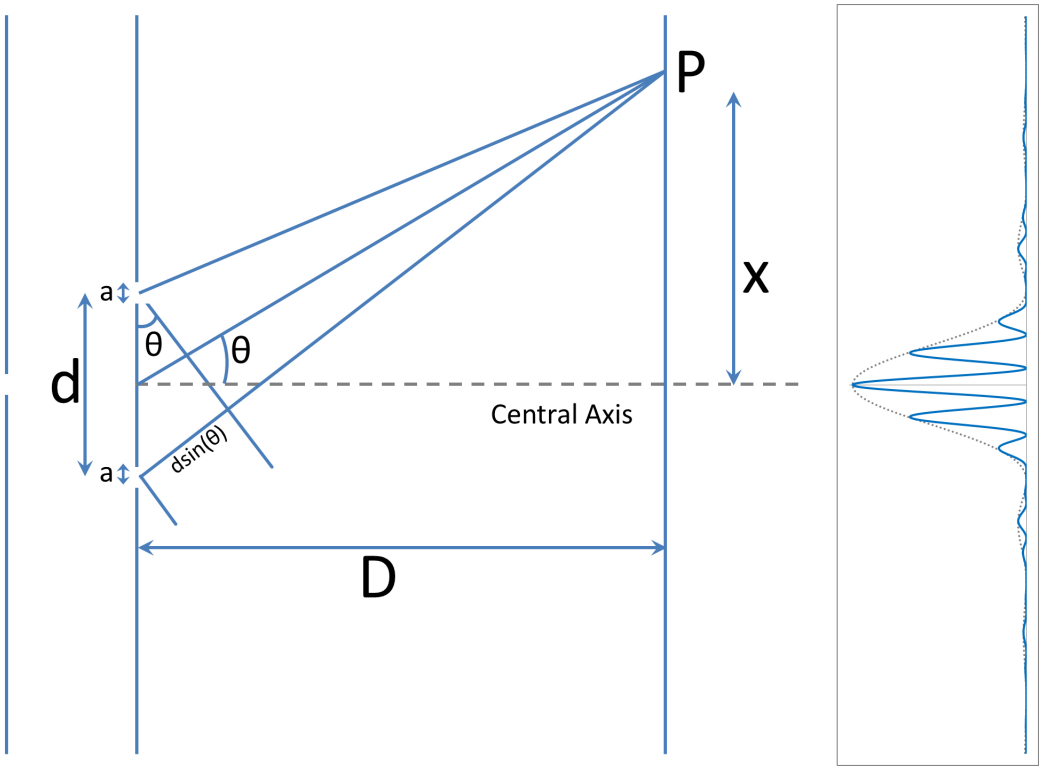

Figure 2.6: Diagram of double slit experiment with intensity profile.

Light passing through any opening, or aperture, will create a diffraction pattern. The diffraction pattern contains spatial frequency information about the aperture. Each area in the diffraction pattern strongly corresponds to a feature in the aperture. If portions of the diffraction pattern are blocked, those features will not be visible in any reconstructed image of the aperture [1].

2.4 Size of Diffraction Pattern Using a Lens

The characteristic size of the diffraction pattern created by a feature in the aperture with a size of d using a lens with focal length f can be found by using Equation 2.27 with $D = f$ and $m = 1$

$$x \approx \frac{f\lambda}{d} \tag{2.30}$$

where x is the lateral distance from the center of the screen to the bright area. This equation gives the location of the chief ray. The feature has a spatial frequency of $\frac{2\pi}{d}$.

2.5 Coherence

If light emanating from different parts of the same wavefront can be made to interfere in a predictable way (as in the double slit experiment), the wave is said to be spatially coherent. If light from different wavefronts can be made to interfere in a predictable way, the light is said to be temporally coherent. Spatially coherent light is required in order to create a diffraction pattern which can be modeled by taking the Fourier transform of the aperture.

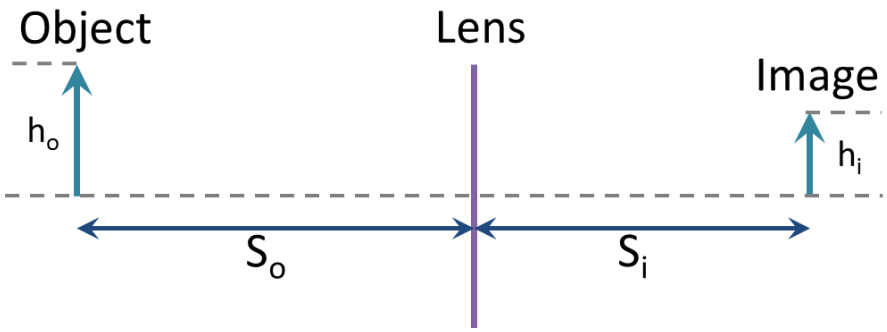

Figure 2.7: An illustration of the Gaussian lens formula, Equation 2.31.

2.6 Image Location and Magnification Calculations

The location of an image produced by a thin lens can be found using the Gaussian lens formula

$$\frac{1}{S_o} + \frac{1}{S_i} = \frac{1}{f} \tag{2.31}$$

where S_o is the location of the object, measured to the left of the lens (if the object is to the right of the lens, S_o has a negative value), S_i is the location of the image, measured to the right of the lens (if the image is to the left of the lens, S_i has a negative value), and f is the focal length of the lens (see Figure 2.7).

To find the location of an image using two lenses, we treat the image from the first lens as the object of the second lens in Equation 2.31 (with S_{i1} as S_{o2}),

$$\begin{aligned} \frac{1}{S_{o_1}} + \frac{1}{S_{i_1}} &= \frac{1}{f_1} \qquad \text{Equation for the first lens} \\ \frac{1}{S_{i_1}} + \frac{1}{S_{i_2}} &= \frac{1}{f_2} \qquad \text{Equation for the second lens.} \end{aligned} \tag{2.32}$$

The magnification of an image can be calculated using the formula for magnification by a thin lens

$$M = -\frac{S_i}{S_o} = \frac{h_i}{h_o} \tag{2.33}$$

where h_o is the height of the object, and h_i is the height of the image. The magnification of a two-lens system is

$$M = \frac{S_{i_1}}{S_{o_1}} \frac{S_{i_2}}{S_{o_2}}. \tag{2.34}$$

A negative value for M indicates the image is inverted [5]. To obtain a specific magnification with a given object distance or focal length, Equation 2.33 can be substituted into Equation 2.31 to obtain

$$\begin{aligned}
\left(\frac{S_o}{S_o}\right)\frac{1}{S_i} + \frac{1}{S_o} &= \frac{1}{f} \\
\left(\frac{S_o}{S_i}\right)\frac{1}{S_o} + \frac{1}{S_o} &= \frac{1}{f} \\
\left(-\frac{1}{M}\right)\frac{1}{S_o} + \frac{1}{S_o} &= \frac{1}{f} \\
\frac{1}{S_o}\left(1 - \frac{1}{M}\right) &= \frac{1}{f}
\end{aligned}$$

which can be rewritten as

$$S_o = f\left(1 - \frac{1}{M}\right). \tag{2.35}$$

Equations 2.35 and 2.31 allow the image location and magnification to be found as a function of the focal length and position of a lens. If the image can be inverted and not affect the outcome, then $|M|$ can be substituted for M and Equation 2.35 becomes

$$S_o = f\left(1 \pm \frac{1}{M}\right). \tag{2.36}$$

This fact will be used later in the calculation of placement of lenses in the apparatus.

2.7 One-Dimensional Fourier Transforms

The Fourier transform is a function which expresses a given spatial function, $f(x)$, in terms of its spatial frequency components. The Fourier transform equation is

$$F(k) \equiv \int_{-\infty}^{\infty} f(x) e^{-ikx}\, dx \qquad \text{Fourier Transform} \tag{2.37}$$

The reverse of this process, the inverse Fourier transform, expresses the spatial frequency components in terms of the spatial distribution. The inverse Fourier transform equation is

$$f(x) \equiv \int_{-\infty}^{\infty} F(k) e^{ikx}\, dk \qquad \text{Inverse Fourier Transform} \tag{2.38}$$

Recall Equation 2.19 which expressed the electric field distribution at the Fourier plane as being proportional to the Fourier transform of the electric field distribution at the aperture. Figure 2.8 shows a plot of a single slit electric field profile and its Fourier transform. The Fourier transform is a sinc^2 function.

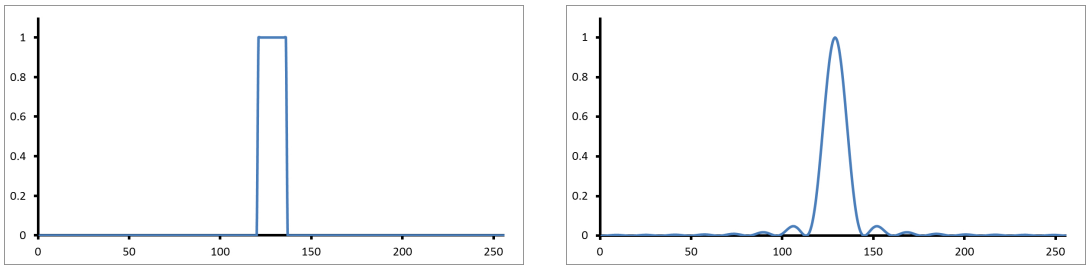

Figure 2.8: A plot of a single slit electric field profile and its Fourier transform.

2.8 Discrete Sampling

Assume a continuous function, $f(x)$, is sampled at regular intervals, Δx, for a finite duration, b. The sampling frequency in this case is $\frac{2\pi}{\Delta x}$. The function $f(x)$ is multiplied by a comb function $h(x)$ to produce a signal $g(x)$

$$g(x) = f(x)h(x) \tag{2.39}$$

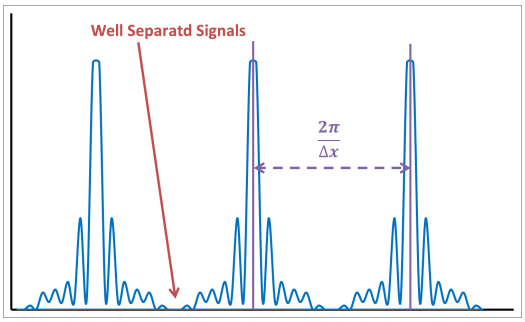

(a) Signal sampled at or above the Nyquist frequency, showing no crosstalk.

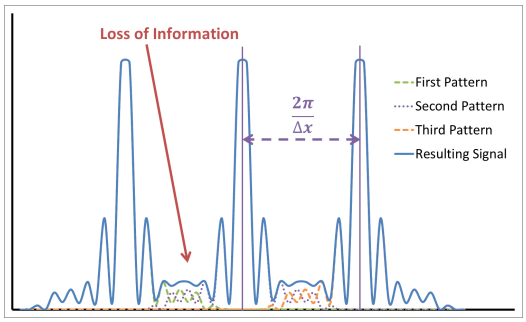

(b) Signal sampled below the Nyquist frequency, showing crosstalk.

Figure 2.9: Signals sampled at or above the Nyquist freqency (a) and below the Nyquist frequency (b).

with

$$h(x) = \sum_{n=1}^{N} \delta(x - n\Delta x) \tag{2.40}$$

where N is the number of samples taken. The function $g(x)$ is the result of two functions multiplied together, $f(x)$ and $h(x)$. When the Fourier transform of $g(x)$ is taken, the Fourier transforms of $f(x)$ and $h(x)$ are convolved (denoted by the symbol $\otimes$) to give

$$G(k) = F(k) \otimes H(k). \tag{2.41}$$

where

$$H(k) = \frac{\sin(k_x b)}{k_x b} \tag{2.42}$$

which is a sinc function with a central peak width of $\frac{2\pi}{b}$.

Discrete sampling results in the Fourier pattern being repeated every $\frac{2\pi}{\Delta x}$ in the frequency domain. If the pattern has spatial frequencies too high, the signal in the frequency domain will contribute to neighboring signals, known as crosstalk, or spatial aliasing (see Figure 2.9). To avoid spatial aliasing, the separation in the frequency domain between the centers of the patterns must obey the relationship

$\frac{\pi}{\Delta x} > \frac{2\pi}{d}$. This can be rearranged to give the relationship

$$2\Delta x > d \tag{2.43}$$

where d is the size of a feature in the function $f(x)$. This relationship implies the sampling frequency must be at least twice as high as the highest spatial frequency present in the sample. This is known as the Nyquist sampling theorem. The Nyquist frequency is one-half the sampling rate. A function can be passed through a low-pass filter to ensure spatial frequencies higher than the Nyquist frequency are not present [6]. Figure 2.10 shows a signal sampled with decreasing Δx values and the central portions of their Fourier transforms. As the sampling rate decreases, the Fourier transforms have less content at higher frequencies.

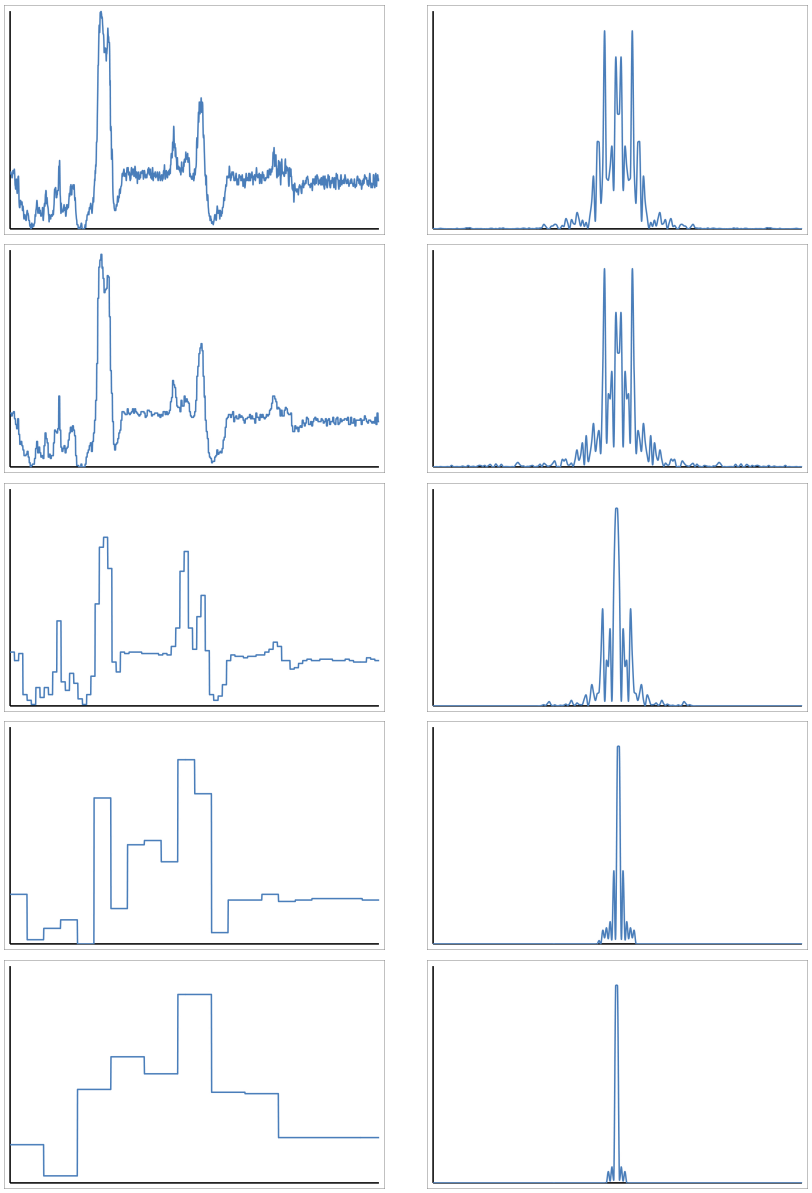

Figure 2.10: A function sampled with different Δx values and the central portion of their corresponding Fourier transforms. As the sampling rate decreases, the Fourier transforms have less content at higher frequencies.

2.9 Two-Dimensional Fourier Transforms

In our apparatus the diffracting aperture is a two-dimensional object mask. As discussed in Section 2.3, the electric field distribution in the diffraction pattern is proportional to the Fourier transform of the object mask. The two-dimensional Fourier transform and inverse Fourier transform equations are

$$F(k_x, k_y) \equiv \iint_{-\infty}^{\infty} f(x,y) e^{-i(k_x x + k_y y)}\, dxdy \qquad \text{2D Fourier Transform} \tag{2.44}$$

$$f(x,y) \equiv \iint_{-\infty}^{\infty} F(k_x, k_y) e^{i(k_x x + k_y y)}\, dk_x dk_y \qquad \text{2D Inverse Fourier Transform} \tag{2.45}$$

Some examples of object masks and their simulated diffraction patterns are presented below. The simulated diffraction patterns are plotted on a logarithmic scale. This is done to prevent small amplitude features from being overwhelmed by much larger amplitude features. The Mathematica code used to generate these simulated diffraction patterns is presented in Appendix A.

Single Slit

The following are examples of single slit diffraction. As the slit widens, the size of the fringes decreases. The slit is a vertical feature in the object mask and is represented as a horizontal feature in frequency space (the diffraction pattern).

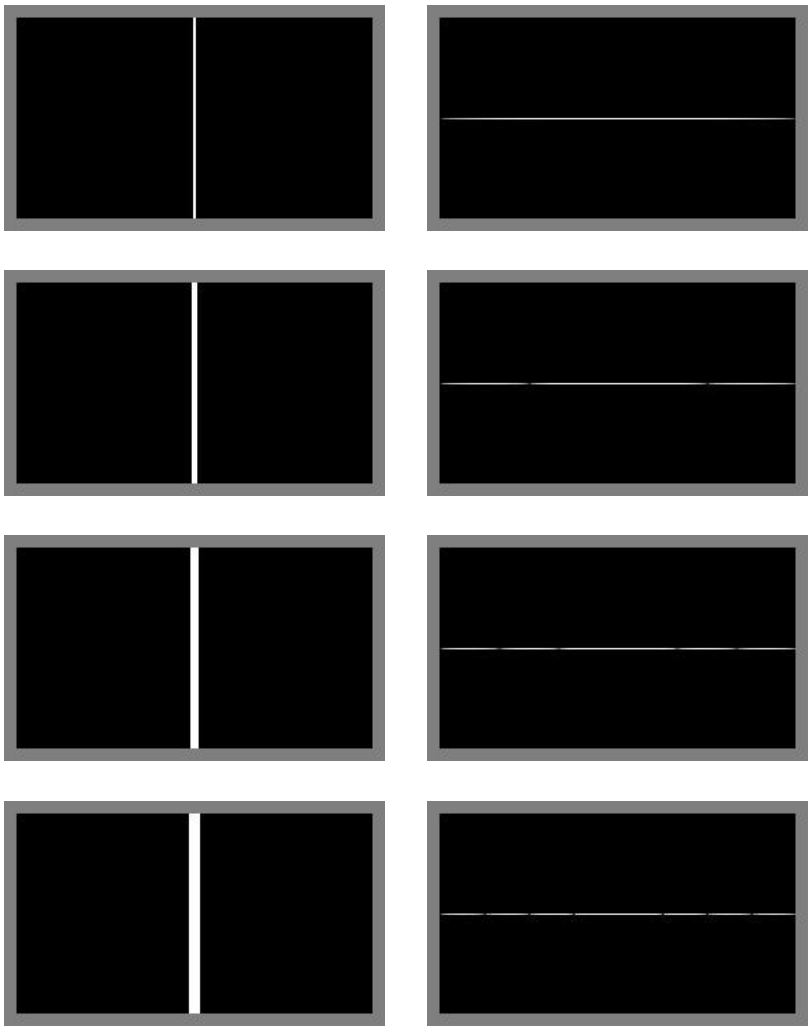

Figure 2.11: Images of a single slit with various widths and their simulated diffraction patterns. As the slit widens, the spacing of the dark fringes decrease.

Rotating Single Slit

Figure 2.12 is an array of a single slit image rotated clockwise and the corresponding simulated diffraction patterns. The horizontal banding structure seen in Figures 2.12b and 2.12d, as well as the the horizontal and vertical smearing of the main lobes of the diffraction pattern in Figure 2.12c, are a result of the finite dimensions of the single slit image.

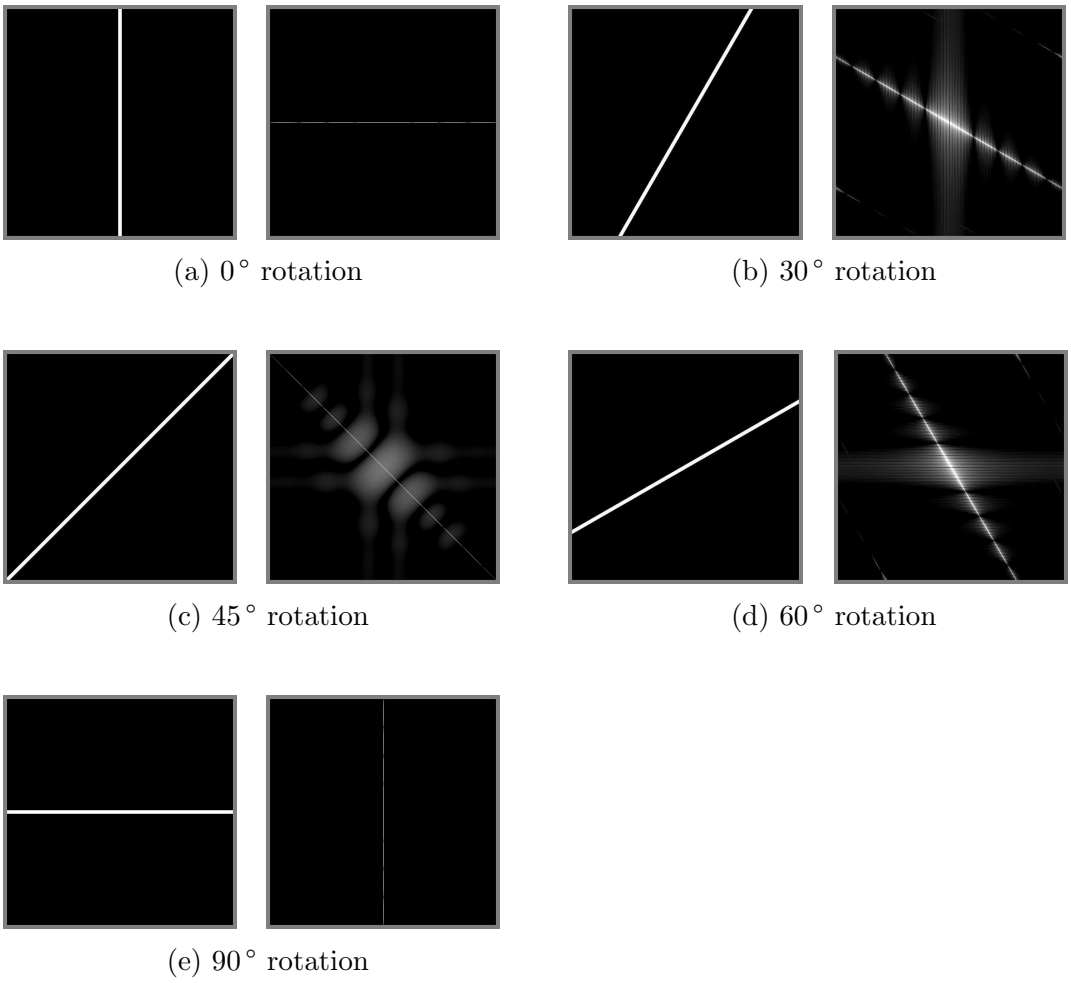

(a) 0° rotation

(b) 30° rotation

(c) 45° rotation

(d) 60° rotation

(e) 90° rotation

Figure 2.12: Single slit images and their simulated diffraction patterns with stated degrees of rotation clockwise from image (a). The horizontal banding structure seen in Sub-figures (b) and (d) as well as the horizontal and vertical smearing of the main lobes of the diffraction pattern in Figure (c) are a result of the finite dimensions of the single slit image.

Circular Apertures

Figure 2.13 shows images of a circle with increasing radii and their corresponding simulated diffraction patterns. As the circle is dilated, the diffraction rings are spaced closer together. The diffraction pattern created by a circular aperture is known as an Airy pattern. The central bright spot is known as the Airy disk [1]. The non-circular lobes are a result of image being rectangular and the image of the circular aperture being pixelated. These lobes are visually exaggerated due to the diffraction pattern being displayed on a logarithmic scale.

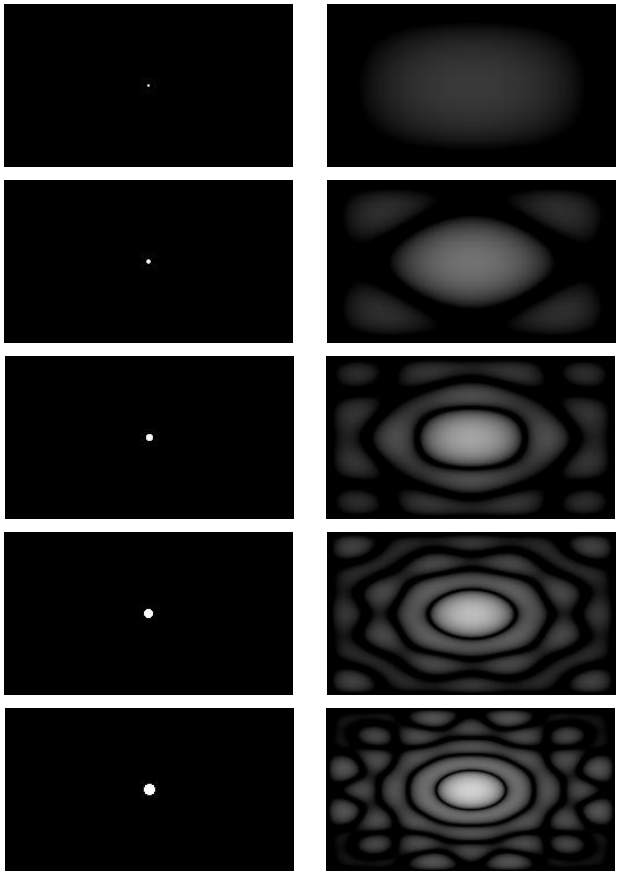

Figure 2.13: Images of a circle with various radii and their simulated diffraction patterns. The non-circular lobes are a result of image being rectangular and the image of the circular aperture being pixelated. The lobes are visually exaggerated in the simulation due to the diffraction pattern being displayed on a logarithmic scale.

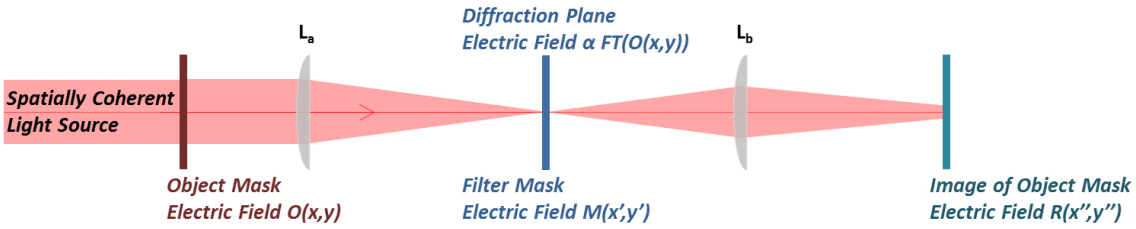

Figure 2.14: Diagram of Fourier filtering experiment with electric fields labeled.

2.10 Spatial Filtering

A system can be constructed where spatially coherent collimated light passes through an object mask. A lens is used to create the Fourier plane, and a second lens is used to image the object mask. At the Fourier plane, filters can be placed to block certain features from appearing in the image of the object mask (see Figure 2.14). This section will examine the electric field as it passes through the system.

Assume a collimated light source passes through an object mask. The amplitude distribution of the electric field after passing through the mask is described by the function

$$O(x, y) \tag{2.46}$$

where $O(x, y)$ is proportional to the square root of the intensity of the light. At the diffraction plane the electric field distribution is proportional to the Fourier transform of $O(x, y)$,

$$O'(x', y') = \iint_{-\infty}^{\infty} O(x, y) e^{-i(k_x x + k_y y)} dx dy \ . \tag{2.47}$$

A substitution using a change of variables can be done

$$k_x \approx k_0 \frac{x'}{f_1} \quad \text{and} \quad k_y \approx k_0 \frac{y'}{f_1} \tag{2.48}$$

to give

$$O'(x', y') = \iint_{-\infty}^{\infty} O(x, y) e^{-i \frac{k_0}{f_1}(x'x + y'y)} dx dy \ . \tag{2.49}$$

The intensity of the pattern is proportional to $|O'|^2$.

A second lens placed after the diffraction plane can be positioned to create an image of the object mask. The electric field at the image plane, $R(x'', y'')$, is proportional to the inverse Fourier transform of the electric field at the Fourier plane. If there are no obstructions, the original function $O(x, y)$ is recovered.

Areas in the diffraction pattern strongly correspond to features in the diffracting aperture (the object mask). By blocking specific areas in the diffraction pattern, the corresponding features will not appear in the reconstructed image of the diffracting aperture. To this end, a filter mask can be introduced at the Fourier plane, which is described by the function $M(x', y')$. The electric field which passes through the Fourier plane is now

$$O'(x', y')M(x', y').$$

The inverse Fourier transform is taken to calculate the electric field distribution at the imaging plane, $R(x'', y'')$, which is

$$R(x'', y'') = \iint_{-\infty}^{\infty} M(x', y') \;\; O'(x', y') \;\; e^{-i(k_x x'' + k_y y'')} \;\; dk_x dk_y \tag{2.50}$$

using the same change of variables shown in Equation 2.48 with

$$dk_x = \frac{k_0}{f_1} dx' \quad \text{and} \quad dk_y = \frac{k_0}{f_1} dy' \tag{2.51}$$

Equation 2.50 becomes

$$R(x'', y'') = \iint_{-\infty}^{\infty} M(x', y') O'(x', y') e^{-i\frac{k_0}{f_1}(x'x'' + y'y'')} \left(\frac{k_0}{f_1}\right)^2 dx' dy' \; . \tag{2.52}$$

These are the calculations for the electric field distribution from the object mask to image plane. The image produced at the image plane is proportional to $|R|^2$.

2.11 Types of Images

As previously stated, features in the diffracting object will create distinct diffraction patterns. Discussion of some typical image features are presented below.

Vertical Features

Vertical features (such as vertical lines) are represented in Fourier space along the horizontal axis. These features can be filtered out using a horizontal line filter as seen in Figure 2.18d. The center of the filter is left open to allow the structure of the rest of the image to pass through.

Horizontal Features

Horizontal features (such as horizontal lines) are represented in Fourier space along the vertical axis. These features can be filtered out using a vertical line filter as seen in Figure 2.18c. The center of the filter is left open to allow the structure of the rest of the image to pass through.

Fractals

A fractal is a self-similar pattern on different scales. One example of a fractal is a Koch Snowflake. The Koch Snowflake was first presented in a paper in 1904 by Helge von Koch. The snowflake is at first an equilateral triangle. One each side, the middle third of the triangle is replaced by a smaller equilateral triangle with the missing piece of the original line serving as its base. This is repeated for all sides. The first four iterations of this process and the simulated diffraction patterns are shown in Figure 2.15. Another example of a fractal is a fractal tree, shown in Figure

2.16 with corresponding simulated diffraction patterns [7] [8].

The finer details in the fractals produce structure further away from the center of the diffraction pattern. Passing a fractal diffraction pattern through a low pass filter blurs the finer detail in the structure of the fractal as can be seen in Figure 2.17.

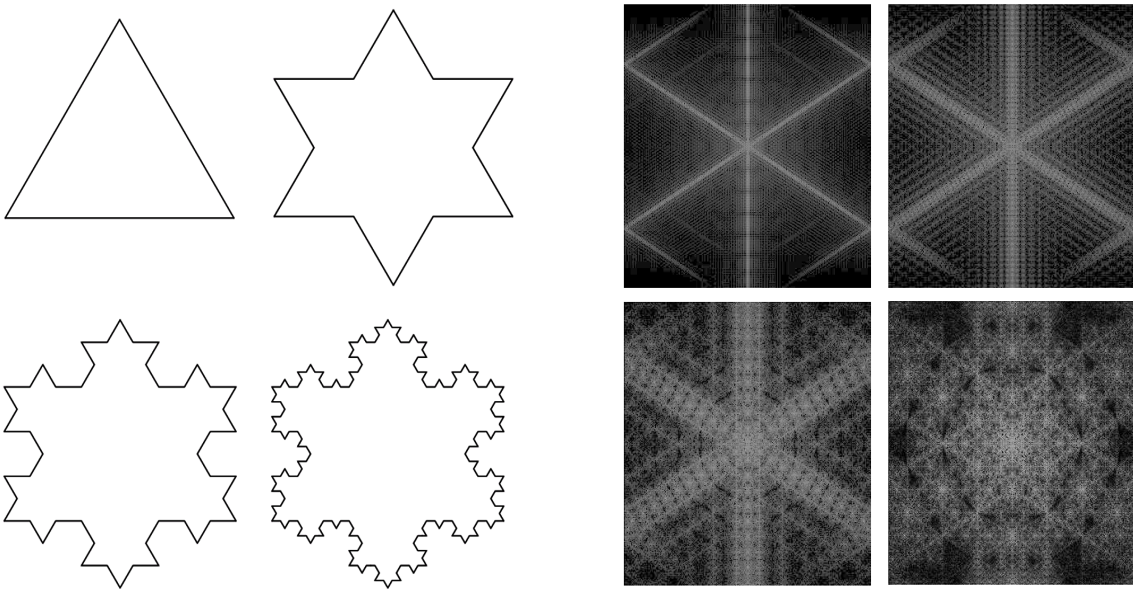

(a) Koch snowflake with 4 different iterations clockwise.

(b) Fourier transform of Koch snowflakes in part (a).

Figure 2.15: Koch snowflake fractals and their simulated diffraction patterns.

2.12 Types of Filters

As previously discussed, filters can be used to block features from appearing in a reconstructed image of an object mask. Discussion of a few types of filters and their uses is presented below. The Mathematica code for generating several of the following filters can be found in Appendix A.

High Pass

A high pass filter allows features with small distances between them, or higher frequency features, to pass but blocks features with larger distances, or lower frequency features. The spatial distance in the object is inversely proportional to the radial distance from the center in the Fourier plane, therefore high frequency features appear in Fourier space in the outer radial areas. A high pass filter is presented in Figure 2.18a. High pass filters can be used to exaggerate the appearance of fine details.

Low Pass

A low pass filter allows features with large distances between them, or lower frequency features, to pass but block features with smaller distances, or higher frequency features. The spatial distance in the object is inversely proportional to the radial distance from the center of the Fourier plane, therefore low frequency features appear in Fourier space near the center of the diffraction pattern. A low pass filter is presented in Figure 2.18b. This type of filter is used on a fractal tree and can be seen in Figure 2.17.

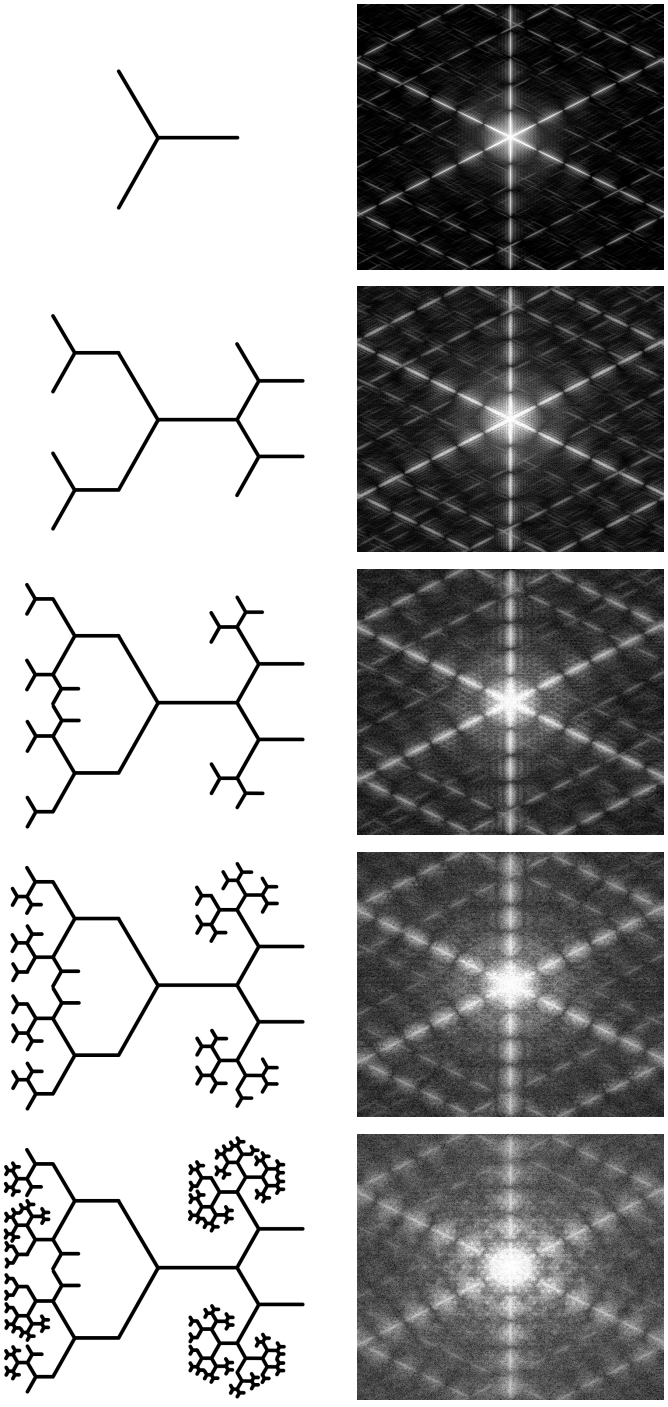

Figure 2.16: Fractal trees with increasing iterations and their corresponding simulated diffraction patterns.

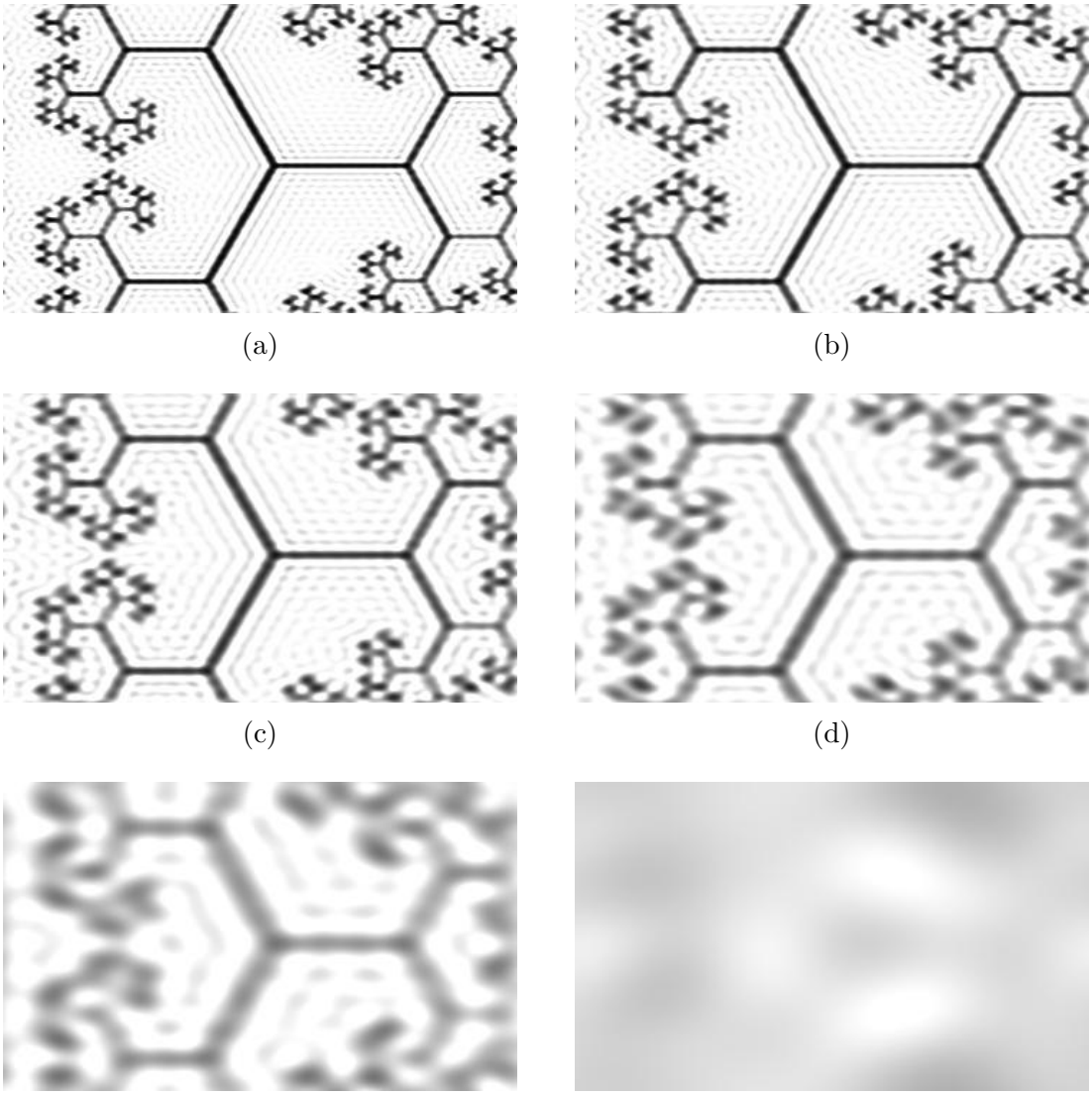

(a) (b)

(c) (d)

(e) (f)

Figure 2.17: Reconstructed images of a fractal tree filtered with a low pass filter, decreasing in radius from (a) to (f).

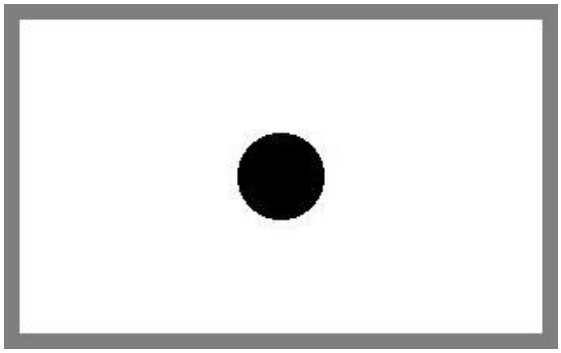

(a) High pass filter.

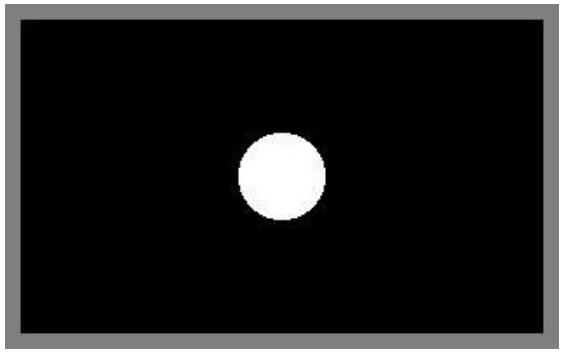

(b) Low pass filter.

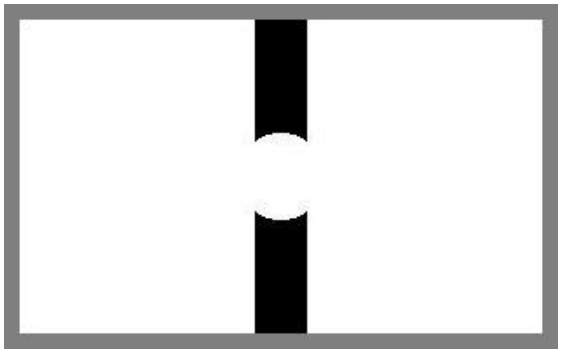

(c) Vertical bar filter.

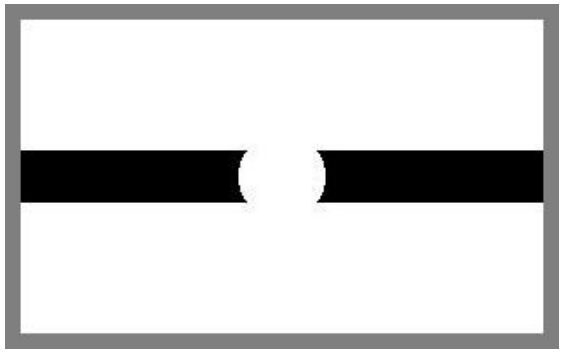

(d) Horizontal bar filter.

Figure 2.18: Various filters generated with Mathematica code.

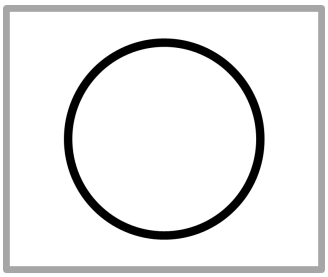

Figure 2.19: An example of a bandpass filter.

Bandpass

A bandpass filter can either block or allow specific spatial frequencies to pass (see Figure 2.19).

Vertical Bar

A vertical bar can be used to block frequencies which represent horizontal features in the diffracting aperture. The center of the filter is left open to allow the structure of the rest of the image to pass through. An example of a vertical bar filter can be seen in Figure 2.18c.

Horizontal Bar

A horizontal bar can be used to block frequencies which represent horizontal features in the diffracting aperture. The center of the filter is left open to allow the structure of the rest of the image to pass through. An example of a horizontal bar filter can be seen in Figure 2.18d.

Specially Tailored

Filters can be created to block very specific features. For example, an image with a grid can have filters created which block only the grid (see Figure 2.20). A specific object mask can be used to filter diffraction patterns of unknown objects in order to determine the presence or absence of a specific feature. This can also be done to determine information in excess of a specific object shape or feature in the object mask.

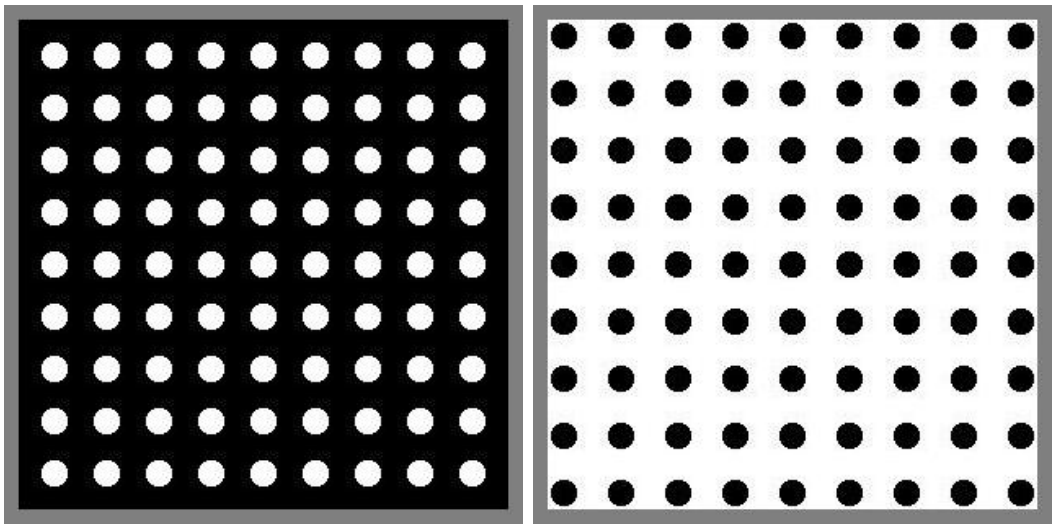

(a) A filter created specifically to allow only a grid in a final image.

(b) A filter created specifically eliminate a grid from a final image.

Figure 2.20: Filters designed for a specific purpose.

CHAPTER 3

DESIGNING THE APPARATUS

An analog Fourier spatial filtering in-class demonstration apparatus was designed and built. The system contains an object and filter which are dynamically changed via computer software and have high contrast values. There are two goals for the apparatus. The first is to spatially filter an image of the object mask. The second is to detect the diffraction pattern created by the object mask. The conceptual optical layout of the apparatus can be seen in Figure 3.1. Spatially coherent light illuminates an object mask and then encounters a beam splitter. At that point the light takes two paths. The first is the spatial filtering portion of the experiment, Path A, which can be seen in Figure 3.2. The second is the path used to image the diffraction pattern, Path B, which can be seen in Figure 3.3.

There are four main components of the experiment: the physical construction, the illumination, the objects and filters, and the detection of both the filtered object and diffraction pattern. Requirements, options, and selections for each of the components are discussed below. A complete list of the parts used in this experiment is presented in Appendix B.

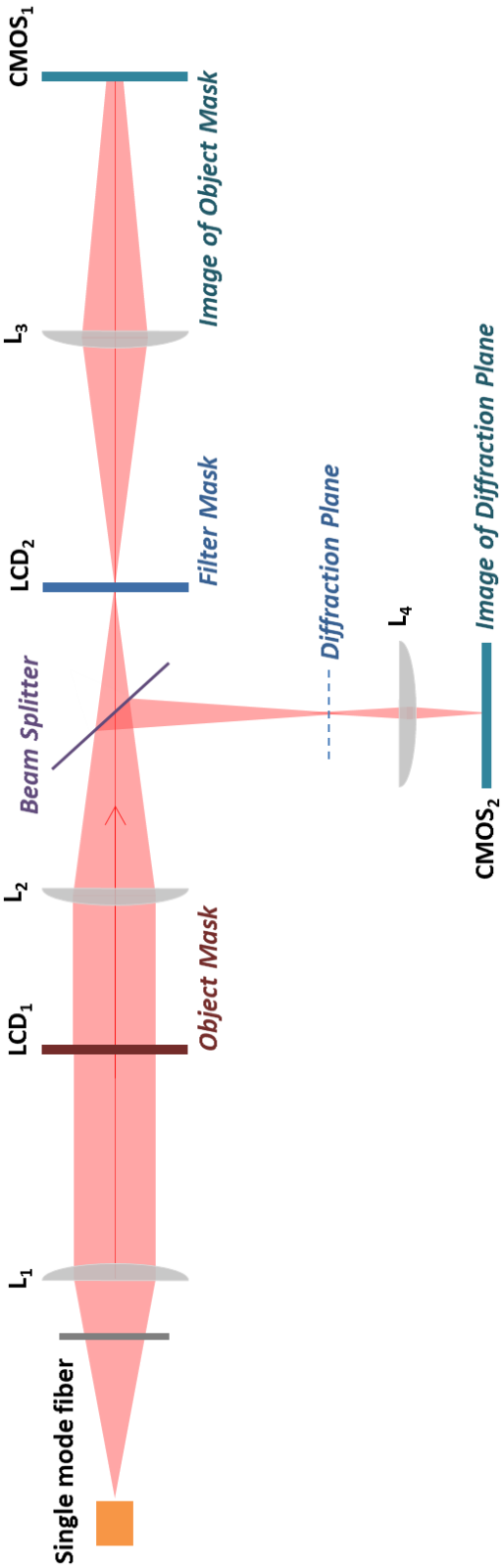

Figure 3.1: Conceptual optical layout of the apparatus.

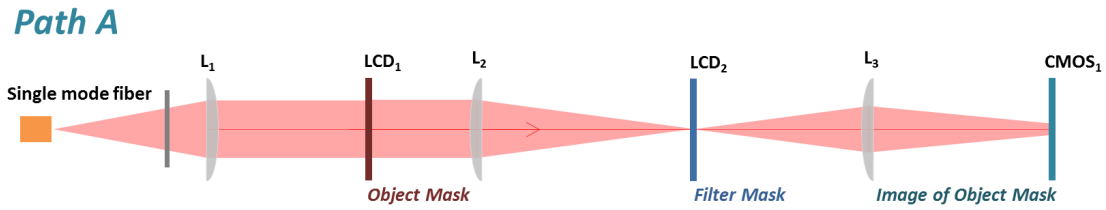

Figure 3.2: Path A shows the spatial filtering path of the experiment.

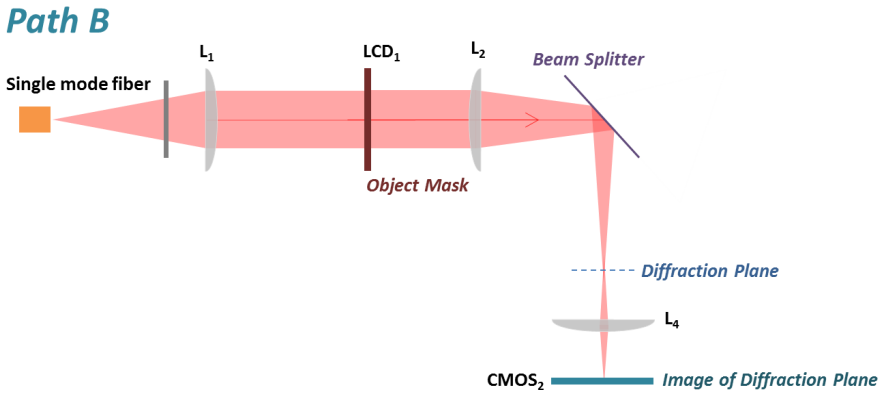

Figure 3.3: Path B shows the path taken to image the diffraction pattern.

3.1 Physical Construction

In regard to the physical construction, the goal was to create a portable experiment, which is easily transported to classrooms. To this end, an available rolling cart and optical bread board were procured. The bread board is 2 ft. × 3 ft. × 6 in. with mounting holes spaced on a 1" grid.

3.2 Illumination

The requirements for illumination are that it: be visible to the human eye, not require special or protective eyewear, and be spatially coherent.

Lasers can produce light which is spatially and temporally coherent. They are classified according to their ability to cause damage to the human eye. Class I lasers are safe to use without protective eyewear. Class II lasers are safe because of the blink reflex. Prolonged exposure is required to cause damage. Class IIa lasers are in the low-powered region of Class II lasers. An exposure of more than 1,000 seconds is required to cause damage by these lasers. Class IIIa lasers are dangerous when combined with optics which change the diameter or power density of the beam [9]. Lasers in Class IIIb and Class IV are very hazardous and should not be used without protective eyewear. For this apparatus, only lasers which are Class I, Class II, or Class IIa would be appropriate. Lasers can be coupled with a single mode fiber to provide light which can be collimated and produce a speckle-free image.

Another option would be a light source which is spatially coherent, but not temporally coherent. A superluminescent diode (SLD) produces such light. An SLD can be packaged with a single mode fiber and be collimated in the same way the laser light is collimated. Since the SLD could be packaged with the single mode

fiber, it would eliminate the need to align the fiber to the light. There are a variety of SLDs which produce light at several different wavelengths.

For our apparatus we chose an available helium-neon (HeNe) laser with an output wavelength $\lambda = 633$ nm of unpolarized light. The laser light is sent through a Thorlabs 2 m single mode fiber suitable for light 600 nm - 800 nm with a numerical aperture of 0.12. The power output at the end of the single mode fiber was measured to be .03 mW, which makes our illumination a Class II fiber-coupled laser. The fiber only transmits one single laser light mode. This creates a clean and spatially coherent beam which is nearly Gaussian. The light emerges from the fiber in a cone. The light is collimated by placing a lens one focal length away from the end of the fiber (L_1 in Figure 3.1). The beam must have spread out enough so that when it is collimated, it will illuminate the entire object mask. Therefore, L_1 in the apparatus is a 2" diameter plano-convex N-BK7 anti-reflection coated glass lens with a focal length $f = 150$ mm. This lens was placed a distance 150 mm from the end of the fiber. Figure 3.4 shows a 30 second exposure of the laser light emerging from the end of the fiber, passing through a polarizer, L_1, and then illuminating the object mask (LCD_1). By collimating the beam we approximate plane wave illumination in the apparatus.

3.3 Objects and Filters

In regard to the objects and filters, it was desirable to have a system in which both are easily changed. It was decided that image display panels from a projector could be used for the object and filter masks. Projector technology was evaluated and is discussed below.

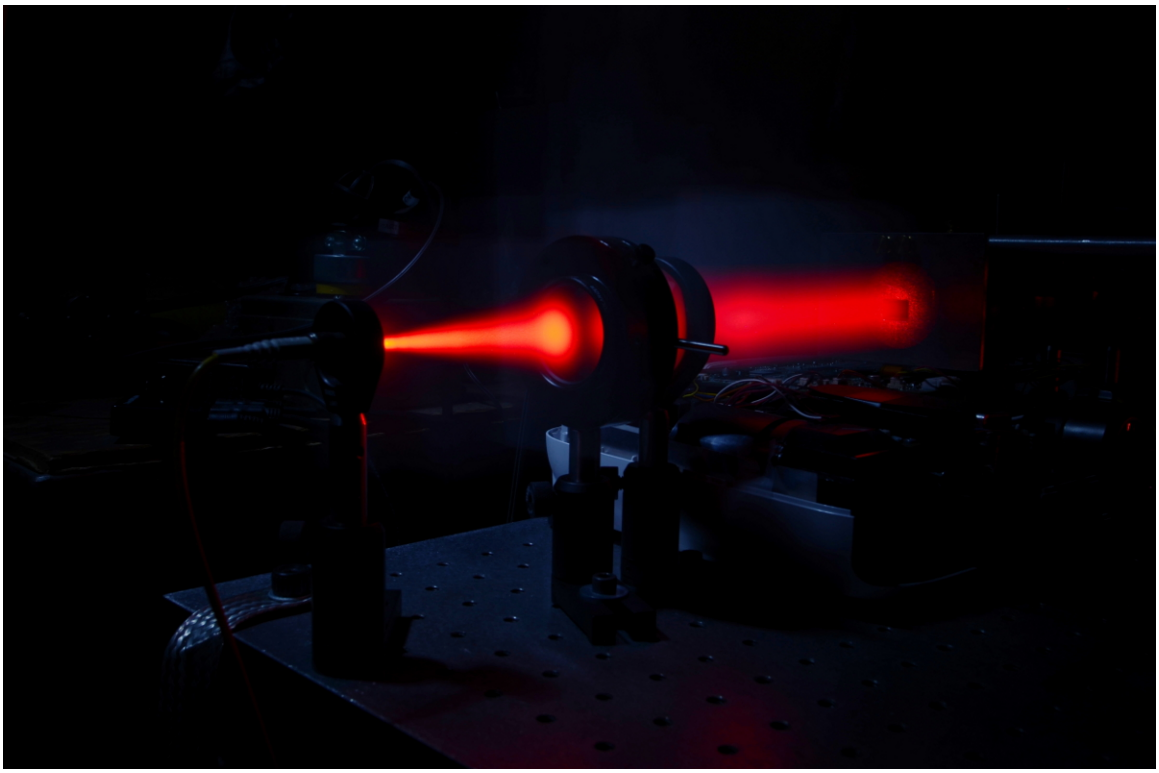

Figure 3.4: Laser light emitted from the end of a single mode fiber passing through a polarizer and collimating lens. The collimated beam then illuminates the object mask.

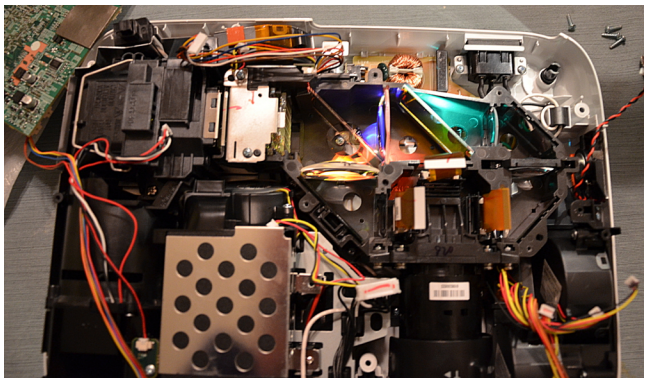

Figure 3.5: An image of the interior of the projector used in this experiment.

Projectors

Three common types of projectors at the time of this writing are: liquid crystal display (LCD), liquid crystal on silicon (LCOS), and digital light processing (DLP). The liquid crystal display (LCD) works by placing polarizers before and after an array of birefringent crystals. The liquid crystal on silicon (LCOS) technology works by reflecting light on a silicon display. The digital light processing technology uses reflections from an array of micro electro-mechanical mirrors.

Only the LCD technology allows a linear light path which is desirable since it allows the experimental setup to most closely match the canonical experimental diagram for Fourier filtering experiments (see Figure 3.1). The projector chosen for this project has three LCD panels in the projector, one each for blue, red, and green light. White light from a halogen bulb is separated using color filters for each of the three colors. The light for each color passes through an initial polarizer, an LCD panel, and a final polarizer. The colors are recombined to form the final image (see Figure 3.5).

It was desirable to create an image with a high pixel fill factor. Projectors were evaluated with available data describing pixel panel size and resolutions. The

panel with the highest pixel fill factor was the Epson PowerLite Home Cinema 705 HD 720p 3LCD Home Theater Projector. This projector has LCD panels which are 12.96 mm × 9.47 mm with a resolution of 1200 × 720. The panels were observed with an optical microscope and have a measured pixel size of 8 μm and a pixel fill factor of 0.8 (see Figure 3.7).

Liquid Crystal Displays

When light travels through media its speed is less than its speed in vacuum. The attribute which describes the speed of light in a material compared to its speed in vacuum is the index of refraction and is defined as

$$n = \frac{c}{v} \tag{3.1}$$

where n is the index of refraction, v is the speed of light through the material, and c is the speed of light in vacuum.

Some materials have different indices of refraction for different polarization directions (sometimes referred to as birefringent material). This results in the E_x and E_y components traveling at different speeds, which could change their relationship and thus change the polarization of the light as it passes through the material (ϕ in Equation 2.2).

The diffracting aperture and spatial filter in this apparatus are LCD panels extracted from two separate projectors. An LCD panel is an array of birefringent molecules. The molecules rotate to align towards an external electric field produced by voltage which is applied via software when images are written to the LCD panel. This changes the polarization of light as it travels through the molecules. A polarizer is placed before the LCD panel to set the initial polarization of the light.

The LCD panel can change the polarization of light to various angles. A second polarizer is placed after the LCD panel and will block light which has had its polarization rotated 90 degrees (see Equation 3.2) [10].

Polarizers

Some devices only allow certain polarization directions to pass through. These devices are called polarizers. For linear polarizers the amount of light which passes through is

$$I(\theta) = I_0 \cos^2 \theta \tag{3.2}$$

where I_0 is the initial intensity, and θ is the angle between the initial polarization of the light and the polarizer. Light which is polarized in the same direction as the polarizer passes through completely. As θ increases, the light passed through is decreased until the polarization of the light and the polarizer are perpendicular and the light is blocked.

Arranging the LCD Panels

Initially, one Epson PowerLite Home Cinema 705 HD 720p home theater projector was purchased. The idea was to use the blue panel as the object mask and the red panel as the filter mask. The LCD panels were extracted from the projector (see Figures 3.6 and 3.7). The blue LCD panel is mounted onto an aluminum plate which also holds a lens, L_2 in Figure 3.1, on center (see Figures 3.8 and 3.9). The LCD panel is connected to the projector via its original flexible printed cable. The location and size of the diffraction pattern created by the LCD panel is determined by the focal length of L_2.

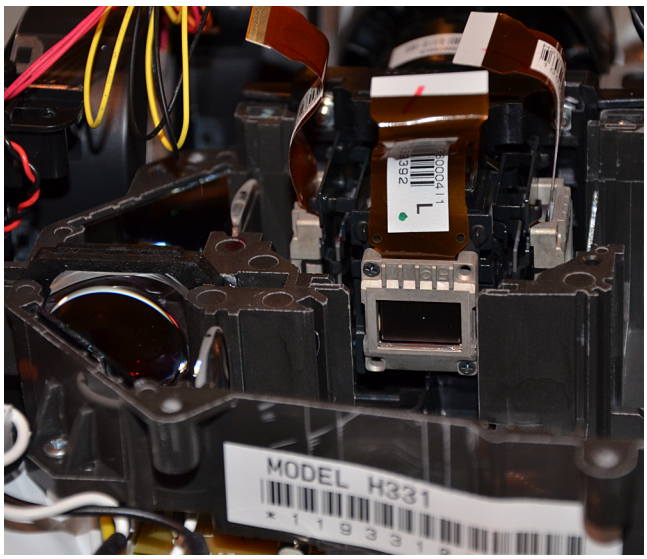

Figure 3.6: An image of an LCD panel in the projector.

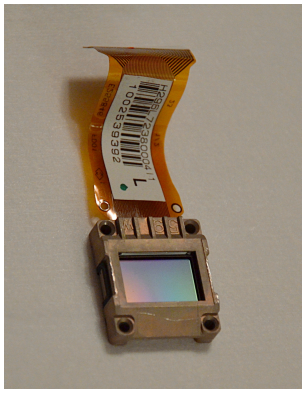

Figure 3.7: An extracted LCD panel.

In the preliminary experimental set up, it was determined that a 5 pixel resolution was reasonable. Any feature smaller than 5 pixels was difficult to discern on the detectors chosen (see Section 3.4).

A diffraction pattern which completely fills the available filter mask area will provide the greatest opportunity for filtering features in the object mask. The filter mask in this apparatus (LCD_2 in Figure 3.1) has an available filter area of 12.96 mm × 9.47 mm. To determine the diffraction size of a 5 pixel feature, Equation 2.30 is used with $y = \left(\frac{1}{2}\right)(9.46 \times 10^{-3}\text{ mm}) = 4.73 \times 10^{-3}$ mm. Rearranging the equation to solve for f we have

$$\begin{aligned} f &= \frac{yd}{\lambda} \\ &= \frac{(4.73 \times 10^{-3}\text{ m})(5)(8 \times 10^{-6}\text{ m})}{(632 \times 10^{-9}\text{ m})} \\ &= 0.3\text{ m} \end{aligned} \tag{3.3}$$

which tells us we should use a lens with a focal length of 300 mm. Therefore L_2 in our apparatus is a 2" diameter plano-convex N-BK7 anti-reflection coated glass lens with a focal length $f = 300$ mm. Since the illumination is collimated, the Fourier plane created by L_2 will be located 300 mm from the lens.

The ribbons connecting the LCD panels to the projector are 76 mm, which was too short for the experiment. A second projector was purchased and positioned so the red LCD panel would be positioned 300 mm from L_2. This LCD panel is the filter mask and labeled as LCD_2 in Figure 3.1. The panel was extracted from the projector and mounted to an aluminum plate which is attached to three translational stages, one each for the x, y, and z axes (see Figure 3.10). The LCD panel is connected to the projector via its original flexible printed cable.

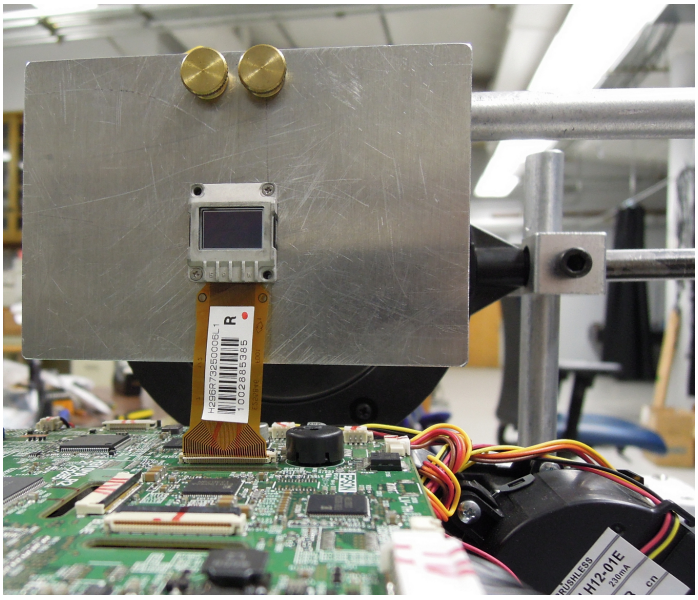

Figure 3.8: An image of LCD_2 mounted on an aluminum plate. Notice the LCD panel is still connected to the projector.

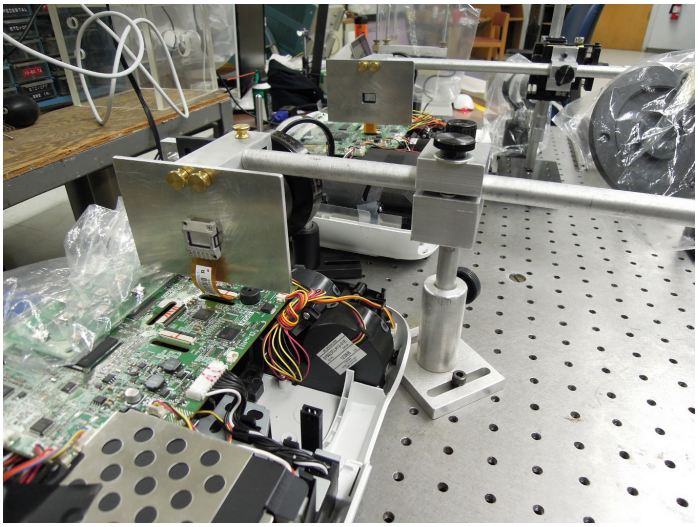

Figure 3.9: LCD_1 mounted on an aluminum block with a 2" diameter lens on center.

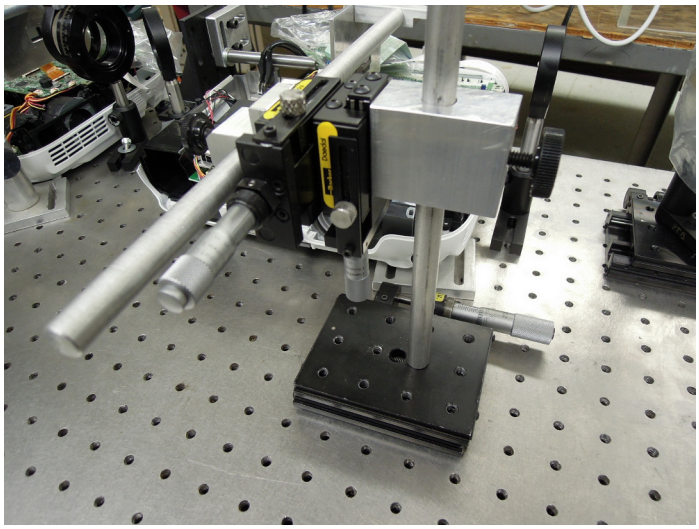

Figure 3.10: LCD_2 mounted on three translational stages for precise control in each axis.

We connected both projectors to one common computer via a passive VGA signal splitter. The blue portion of the signal is displayed on LCD_1, and the red portion of the signal is displayed on LCD_2. Images can be written to the projectors in the same way they are written to in standard uses. We are using custom, open source software developed by Troy Fisher to drive the projectors [11]. The software writes independent monochrome images to the blue and red channels in the video signal.

The original light source, a halogen lamp, was removed from each projector. It was unnecessary and created light pollution in the apparatus. This model of projector shuts down if it senses the light source is not functioning properly. To prevent this automatic shutoff, the presence of the light source is simulated with a dummy load in the form a 30 Ω 200 W power resistor. Two insulated copper wire bundles are used to connect a resistor to the each of the projectors. One end of the copper bundle is soldered onto each power resistor terminal. The other end is soldered to a metal prong. The prongs are inserted into the projector where the connectors for the lamp are situated (see Figure 3.11). Two unused computer power cords were the source of the insulated copper wire bundles. The resistors produce 200 W of heat. To help dissipate heat, they are mounted on large aluminum plates with large cooling fins to the underside of the optical bread board (see Figure 3.12).

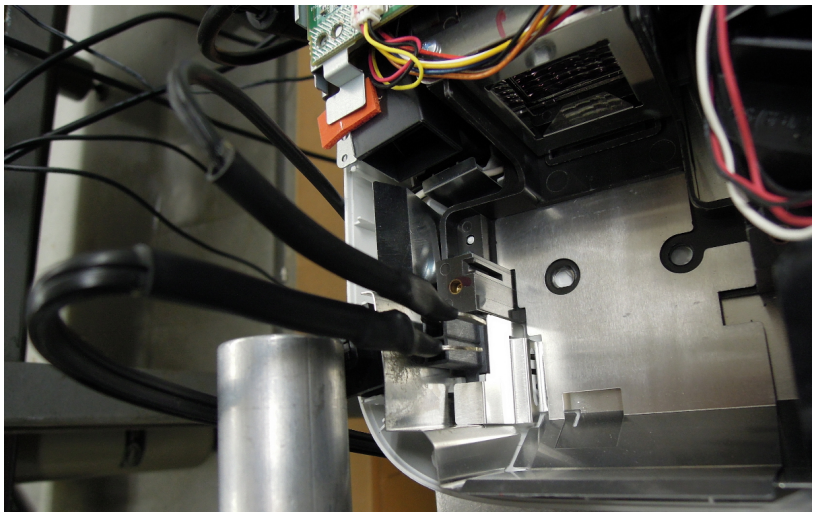

Figure 3.11: Metal prongs inserted into a projector where the lamp is usually situated. The prongs are soldered to one end of an insulated copper wire bundle. The other end of the wire bundle is soldered to a 30 Ω 200 W power resistor.

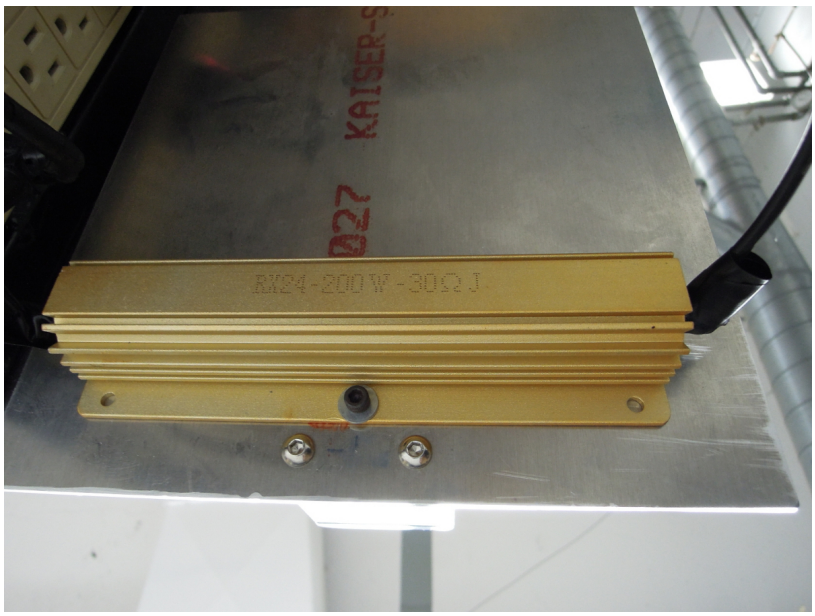

Figure 3.12: A 30 Ω 200 W power resistor mounted onto aluminum plate, which is mounted onto the rolling cart. The resistor provides a dummy load to run the projector without the original lamp.

An LCD panel works by spatially modulating the polarization of light. To convert this into amplitude modulation for a visible image, polarizers must be placed before and after the panel. The projector has polarizers before and after each LCD panel. However, since we have removed the LCD panels from the projectors we must place polarizers in the light path before and after each LCD panel. A polarizer set to 0° is placed before L_1 in our apparatus to provide initial polarization for the illumination. A second polarizer set to 0° is placed after LCD_1 to create the object image. The image produced is the negative of what appears on the screen. If one of the first two polarizers were set to 90° then the image would be as it appears on the screen. A third polarizer set to 65° is placed after LCD_2 to allow only the filtered image through.

3.4 Image and Diffraction Detection

It was desirable to use a computer to view both the image of the filtered object mask and the diffraction pattern. Two Logitech C525 webcams were purchased and their optics were removed to expose the CMOS sensors. The sensors are used to collect the image of the filtered object and the diffraction pattern from the object. The power indicator light was de-soldered from the board, as it was causing light pollution in the apparatus [12]. The CMOS sensors are 3.8 mm × 2.8 mm. The remaining body from the webcam is mounted using an optics holder and post which is inserted into an optical mount and screwed into the optical bread board (see Figure 3.13).

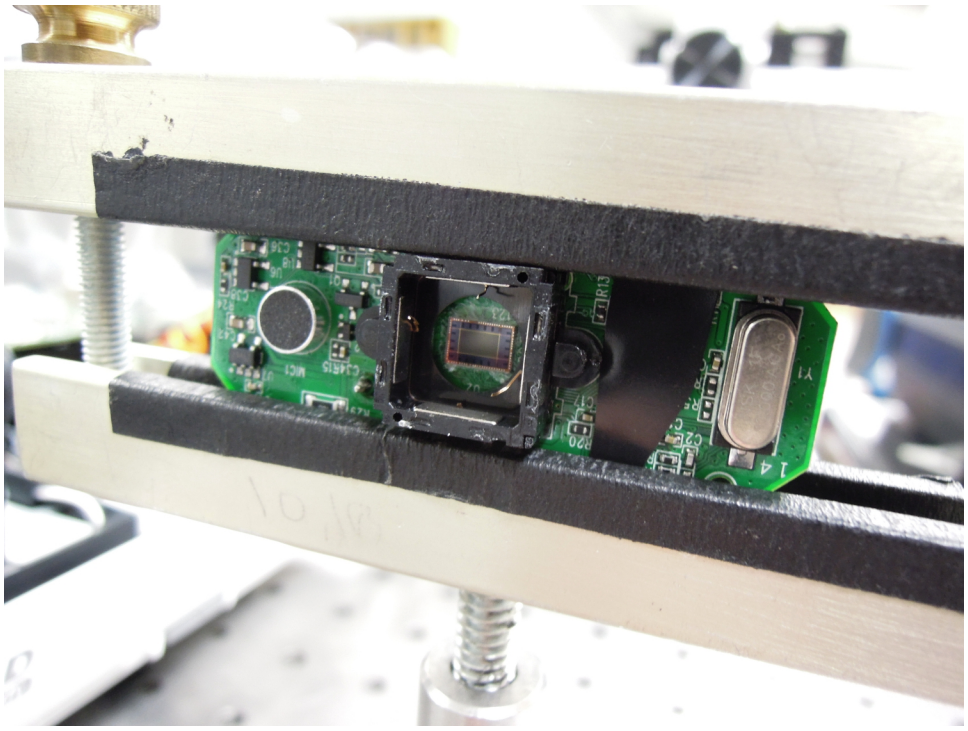

Figure 3.13: An exposed CMOS sensor measuring 3.8 mm × 2.8 mm from a Logitech C525 webcam. The power light indicator was de-soldered from the board [12].

To create the filtered image of LCD_1 onto $CMOS_1$ a lens is used (L_3 in Figure 3.1). The LCD panels have a vertical height of 9.47 mm. The CMOS detectors have a vertical height of 2.8 mm. This means the magnitude of the magnification should be

$$M = \frac{h_i}{h_o} = \frac{2.8 \text{ mm}}{9.46 \text{ mm}} = 0.3. \tag{3.4}$$

The magnification of a two lens system is

$$M = \frac{S_{i1}}{S_{o1}} \frac{S_{i2}}{S_{o2}}. \tag{3.5}$$

A lens with a short focal length was chosen in order to constrain Path A to the 914 mm length of the optical bread board. Therefore, L_3 is a plano-convex N-BK7 anti-reflection coated 2" diameter lens with focal length $f = 100$ mm. Equations 3.4, 3.4, and 2.35 are used to find the appropriate placement of L_3 (124 mm from LCD_2). Figures 3.14 and 3.15 show images of the laser light diffracting through LCD_1 and illuminating LCD_2. The multiple beams are a result of higher order diffraction caused by the pixels in LCD_1.

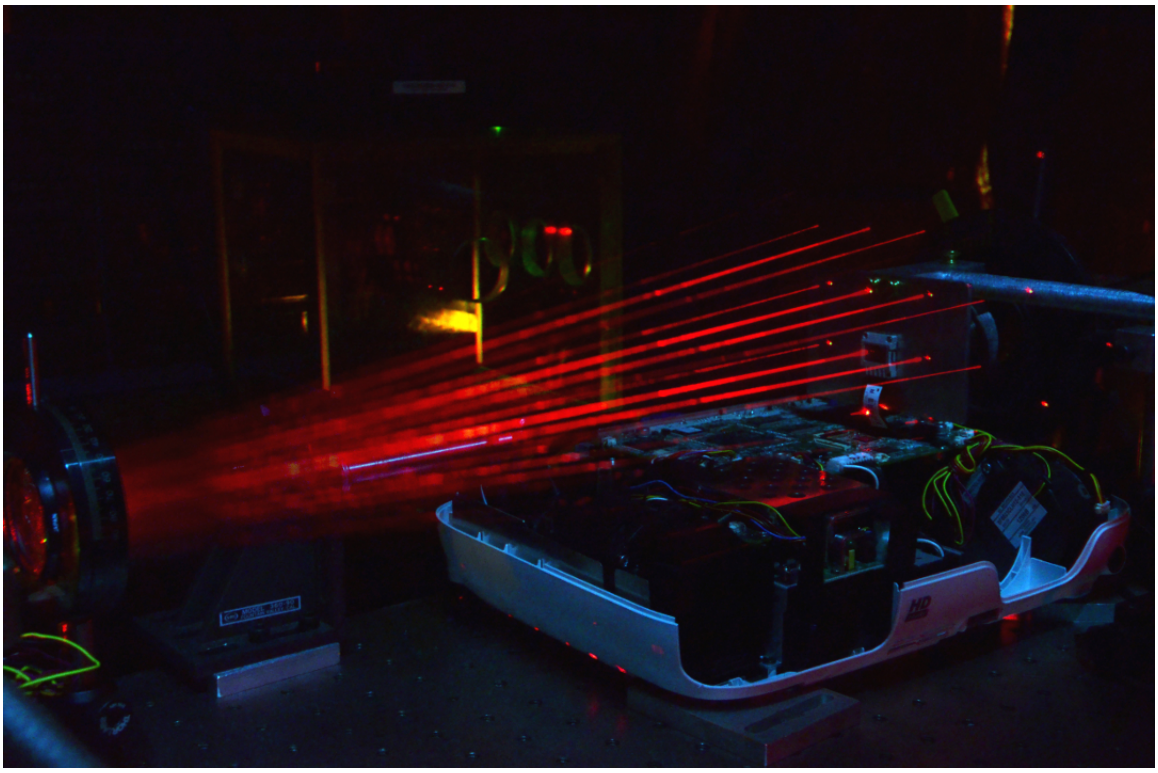

Figure 3.14: The laser light diffracts through the object mask (LCD_1) and illuminates the filter mask (LCD_2). The multiple beams are higher-order diffraction caused by the pixels in LCD_1.

Figure 3.15: Close up image of diffracted light from the object mask (LCD_1) illuminating the filter mask (LCD_2). The multiple beams are higher-order diffraction caused by the pixels in LCD_1

We also wish to view the diffraction pattern of the image displayed on the object mask. To accomplish this a beam splitter is introduced into the light path between the second polarizer and LCD_2. A beam splitter will partially reflect and partially transmit light. The transmitted portion is used to image LCD_1, and the reflected portion is used to view the diffraction pattern created by the image written to LCD_1.

L_2 was chosen for the purpose of creating a diffraction pattern which would fill the vertical space of LCD_2. In order to image this diffraction pattern on $CMOS_2$ a magnification of $|M| = 0.3$ is required. Another lens, L_4 in Figure 3.1, is used to accomplish this. L_4 is a 2" diameter plano-convex N-BK7 anti-reflection coated glass lens with a focal length $f = 150$ mm. In order to conserve space, a lens with a short focal length of $f = 100$ mm was chosen. Equation 2.36 is used with the required value of $|M| = 0.3$, which gives $S_o = 433$ mm. Equation 2.31 is used to find the location of $CMOS_2$ ($S_i = 130$ mm).

We have done what we set out to do. A portable spatial filtering apparatus was built. The object and filter masks are easily changed. Open source software both writes images to the object and filter masks and collects images from CMOS sensors. Table 3.1 lists the lenses used in this apparatus. All of the lenses are 2" diameter plano-convex BK7 glass lenses with an anti-reflection coating. Table 3.2 lists the sizes and attributes of various components used in this apparatus. Figure 3.16 is a diagram with details of the chosen components and their placement.

Table 3.1: Component Sizes

Component	Size
Wavelength	633 nm
Size of LCD Panel	12.96 mm × 9.47 mm
Size of Pixel	8 μm
Size of CMOS	3.81 mm × 2.81 mm

The sizes of components used in the experiment.

Table 3.2: Lenses

Lens	Function	focal length f (mm)
L_1	Collimate the laser beam	150
L_2	Create diffraction plane from LCD_1	300
L_3	Image LCD_1 onto $CMOS_1$	100
L_4	Image diffraction plane onto $CMOS_2$	150

Table of the lenses used in the experiment. All lenses are 2" diameter plano-convex BK7 glass lenses with an anti-reflection coating.

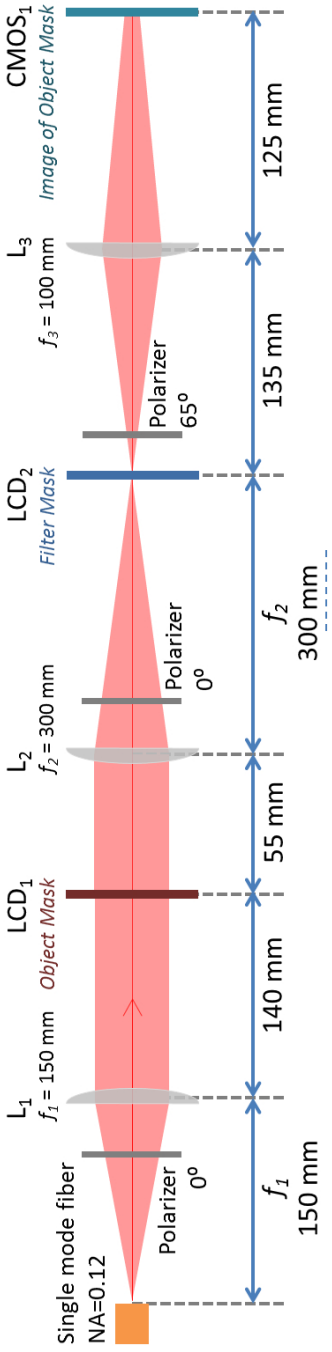

Figure 3.16: Diagram of the apparatus with dimensions and polarizer positions.

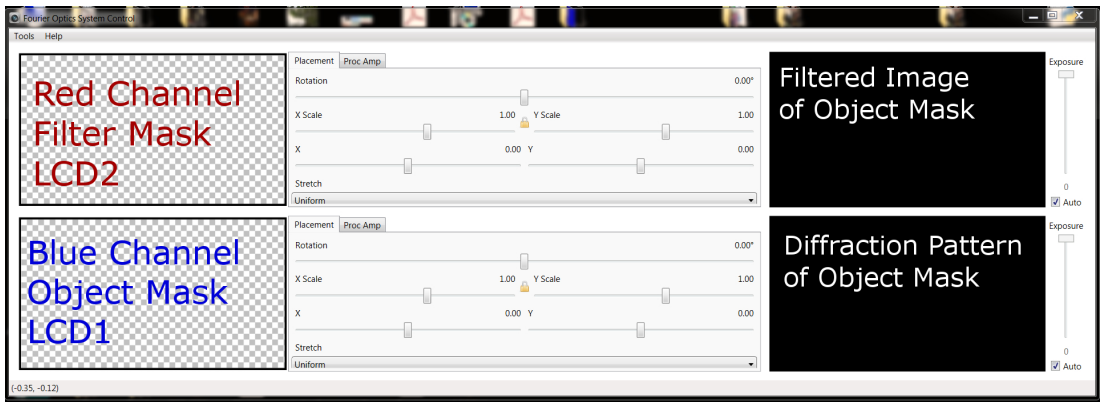

Figure 3.17: Screen capture of Fourier Optics System Control software being used for the apparatus with displays and video input areas labeled.

3.5 Results

A screen capture of the custom Fourier Optics System Control (FOPSC) software with the output and input areas labeled is shown in Figure 3.17. This software writes monochromatic images to the red and blue channels, has some controls for image manipulation, and has two displays for video inputs. In the apparatus built, the blue channel is written to the object mask, and the red channel is written to the filter mask. This arrangement can be reversed, depending on how the apparatus is constructed. The displays for the video inputs are easily changed in the software (i.e., the diffraction pattern can be displayed on the top or bottom window). The labeled inputs are a typical arrangement; however they are not static. The window resizes the components whenever it is resized, which accounts for the different appearance of the window in the following figures.

Collected Diffraction Patterns

Figure 3.18 shows images of single slits with various widths written to the object mask (LCD_1) and the diffraction patterns recorded on $CMOS_2$. The lens L_2 for these images had a focal length of 500 mm. The images were digitally enhanced to make the filtered image more visible. The image for the object mask is file name "Filters 07.jpg" available in the "Filters" menu. The width of the slit was adjusted using the image manipulation controls to the right of the image display window.

Figure 3.19 shows an image of a single slit which was rotated and the collected diffraction pattern. The image was digitally enhanced and cropped from a screen capture to make the diffraction pattern more visible.

Figure 3.20 shows various circular images written to the object panel and the diffraction pattern collected on $CMOS_2$. These images were cropped from a screen capture of the FOPSC software. The lens L_2 for these images had a focal length of 500 mm. The images were digitally edited to enhance the visibility of the diffraction pattern. Several circular filter images are included with the software. Files named "Filters.01.jpg," "Filters.02.jpg," "Filters.03.jpg," and "Filters.04.jpg" available in the "Filters" menu are images of circles with various radii. Some of these were written to the object mask to simulate a circular aperture. Some of the images were scaled, creating an image which appears more like a polygon than a circle. The non-circular structures in the diffraction patterns are due to the straight edges in the image.

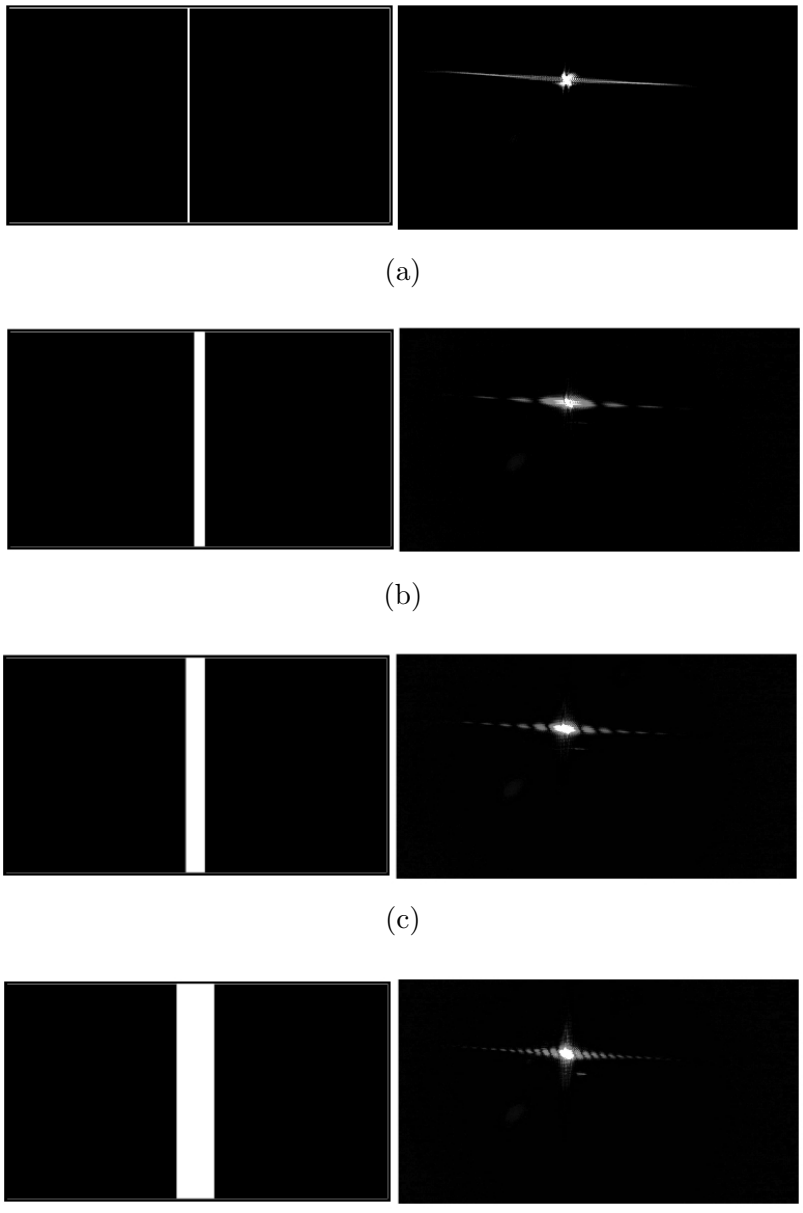

(a)

(b)

(c)

(d)

Figure 3.18: Collected diffraction patterns of single slits with various widths. The images were digitally enhanced to make the filtered image more visible.

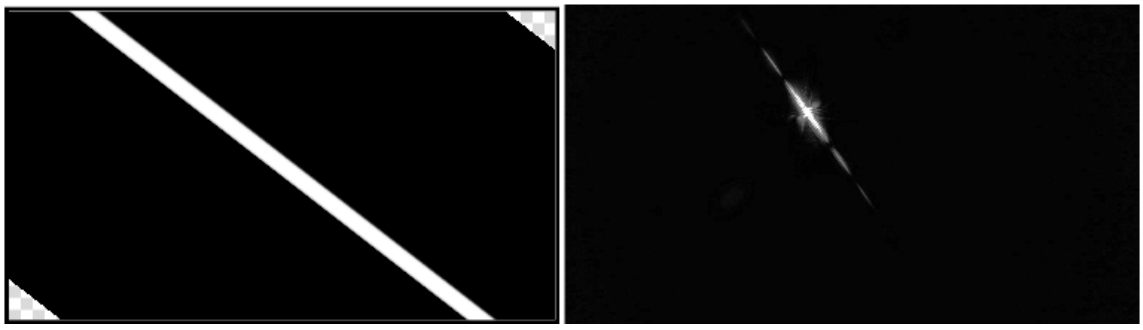

Figure 3.19: Collected diffraction pattern of a rotated slit. The images were cropped from a screen capture and digitally enhanced to make the diffraction pattern more visible.

Figure 3.21 shows images of rings which were written to the object mask and their collected diffraction patterns (from $CMOS_2$). The images were files named "20 circles.jpg" and "60 circles.jpg" available in the "Images" menu in the software. The lens L_2 for these images had a focal length of 500 mm. The images were digitally edited to enhance the visibility of the diffraction patterns.

Figure 3.22 shows images of fractal trees with five iterations and their recorded diffraction patterns. The lens L_2 for these images had a focal length of 500 mm. The images were cropped and digitally enhanced to make the diffraction patterns more visible.

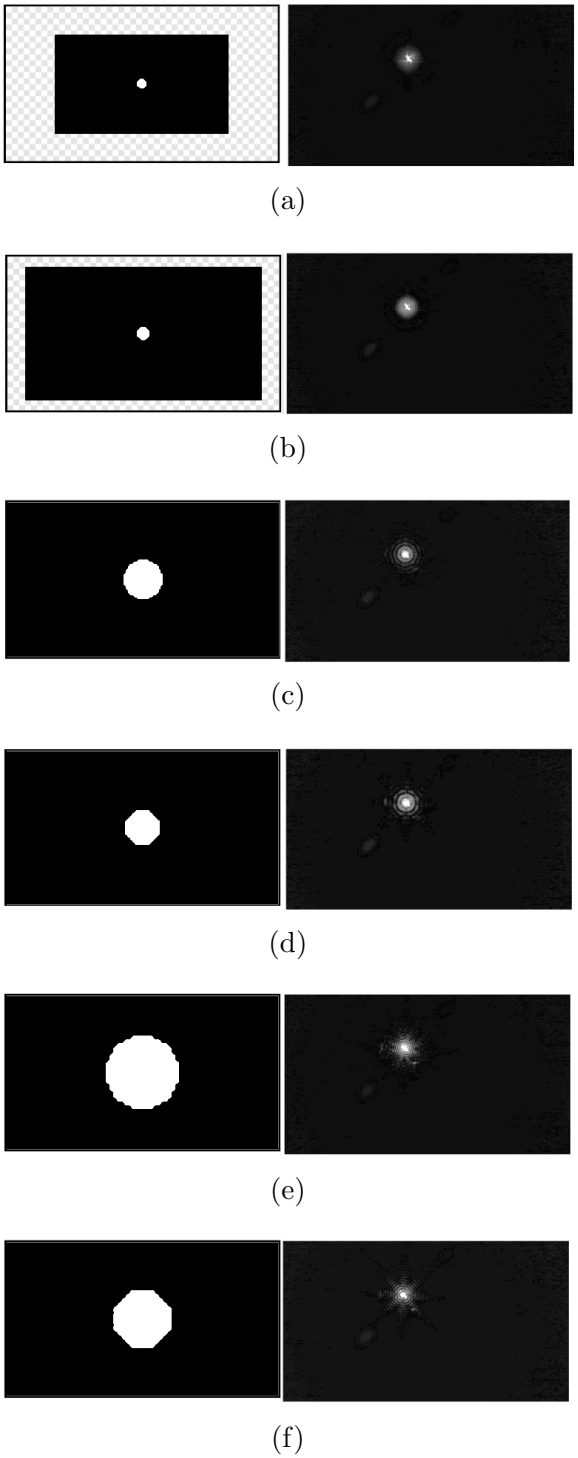

(a)

(b)

(c)

(d)

(e)

(f)

Figure 3.20: Collected diffraction patterns of various images of circles. As the image of the circle begins to resemble a polygon, the diffraction pattern contains more non-circular features. The images were digitally enhanced and cropped from screen captures to make the filtered image more visible.

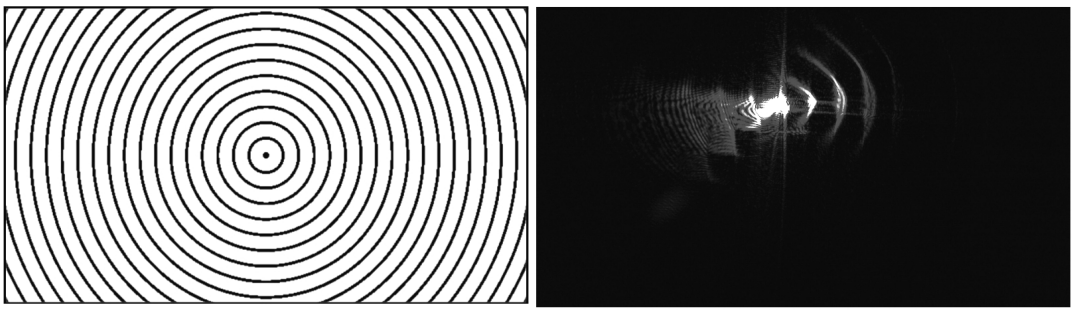

(a)

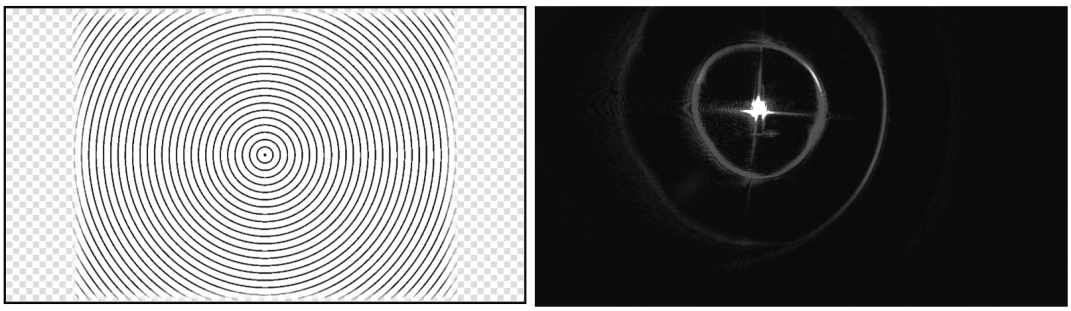

(b)

Figure 3.21: Collected diffraction patterns of images of rings. The images were cropped from screen captures and digitally edited to enhance the visibility of the diffraction patterns.

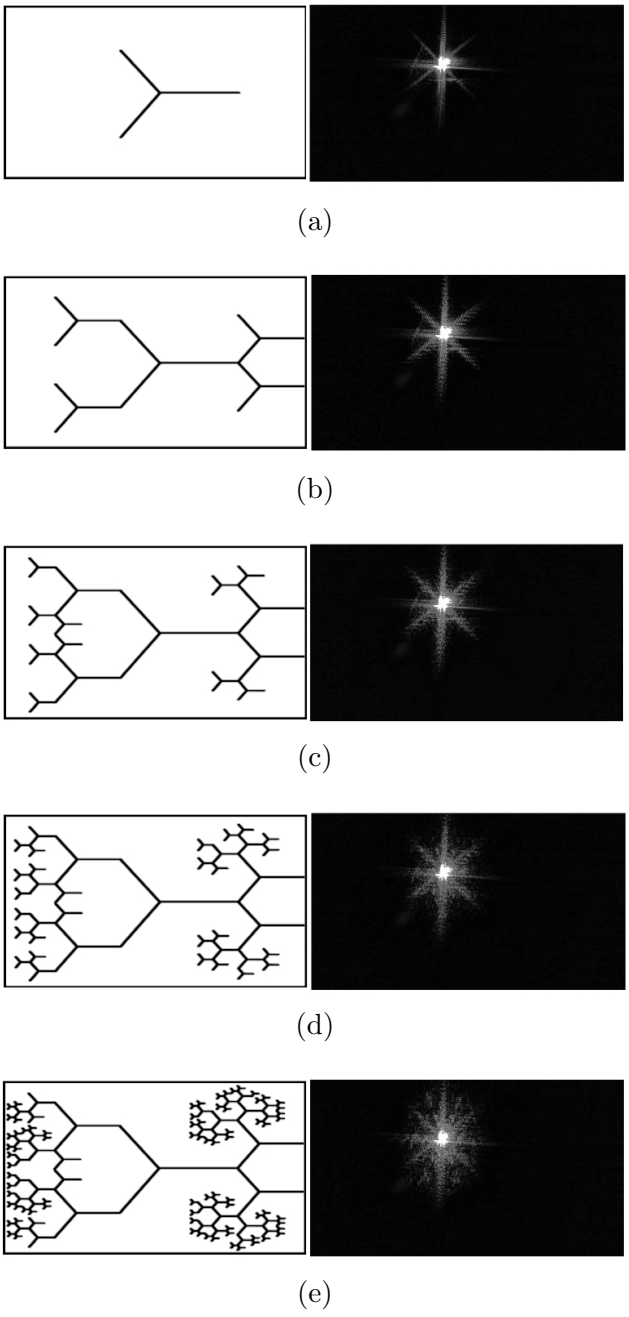

(a)

(b)

(c)

(d)

(e)

Figure 3.22: Collected diffraction patterns of fractal trees with various iterations. The images were cropped and digitally enhanced to make the filtered image more visible.

Successful Spatial Filtering of Vertical Lines

Successful spatial filtering of vertical lines is presented in Figure 3.23. An image of vertical lines, file name "20 Vertical Lines.jpg" under the "Images" menu in the software, is written to the object mask. A complete vertical bar filter, file name "Filters.07.jpg" under the "Filters" menu is written to the filter mask. The filter is initially mis-aligned to allow the diffraction pattern through the system. The filter is then aligned in order to block the vertical structure pattern (represented on the horizontal line in the diffraction plane). These images were acquired without a beam splitter in the light path.

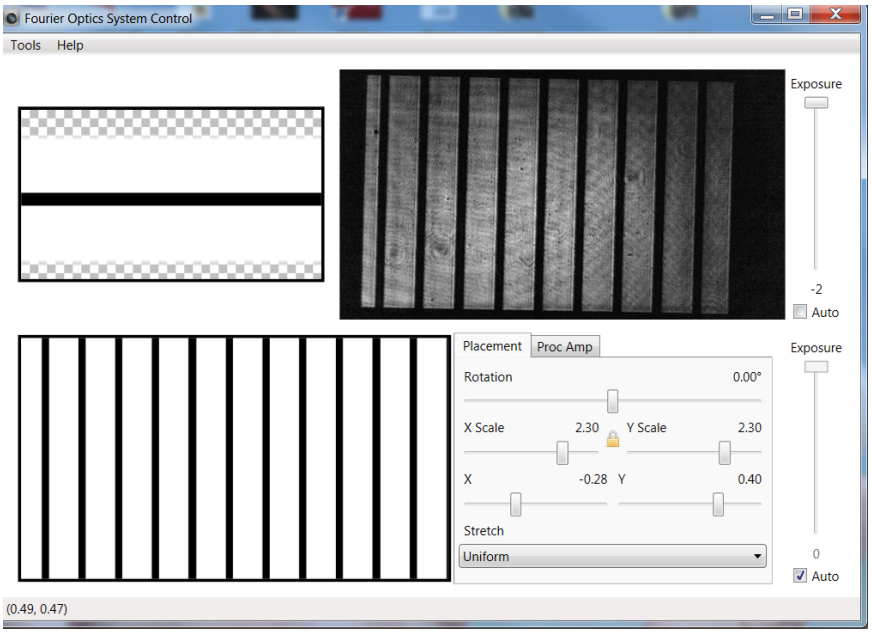

(a) Filter not aligned correctly allows the diffraction pattern to pass through the Fourier plane.

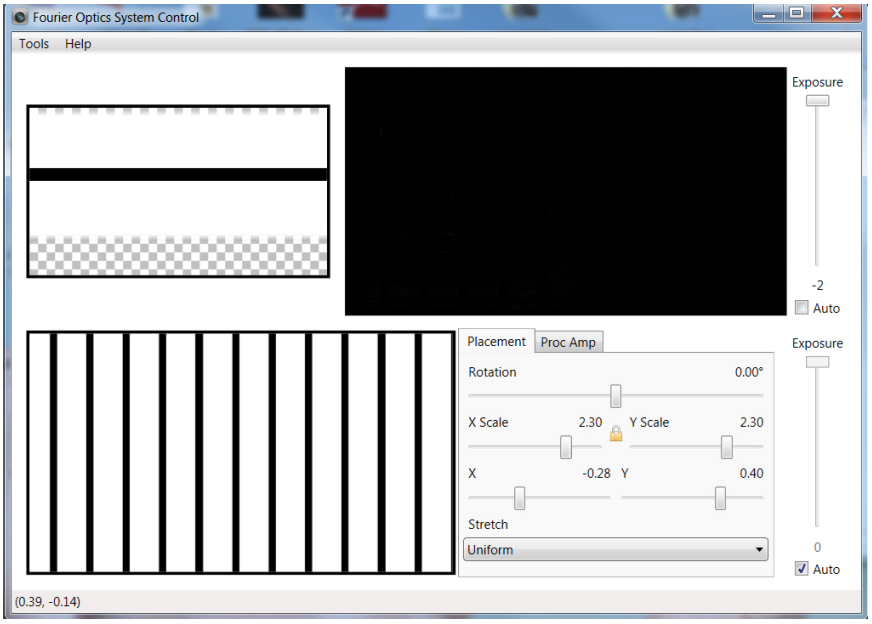

(b) Filter aligned correctly does not allow the diffraction pattern to pass through the Fourier plane.

Figure 3.23: Screen capture of FOPSC software showing the image of LCD_1 (collected on $CMOS_1$) with and without spatial filtering. The image written to the filter mask was adjusted through the software controls until the vertical lines disappeared from the reconstructed image.

Successful Spatial Filtering of a Fractal Tree

Another example of successful spatial filtering is presented in Figure 3.24. An image of a fractal tree was written to the object mask (LCD_1). A low pass filter was written to the filter mask (LCD_2). The size of the filter was adjusted using the image controls to the right of the filter mask window. The reconstructed image detected on $CMOS_1$ is shown in the upper right video input window. The lens L_2 for these images had a focal length of 500 mm. The screen captures were digitally enhanced to make the filtered image more visible.

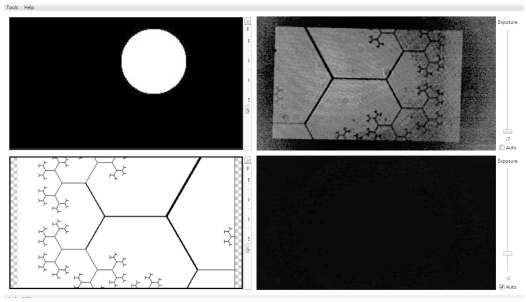

(a)

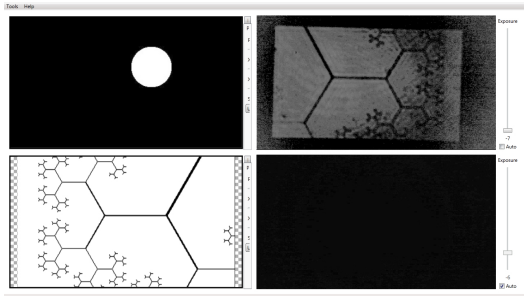

(b)

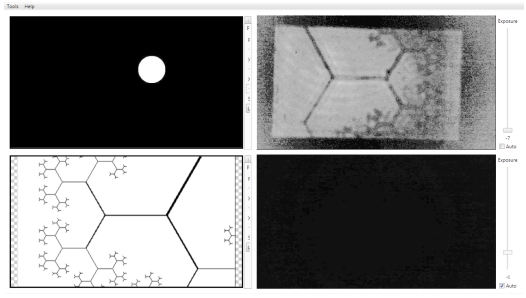

(c)

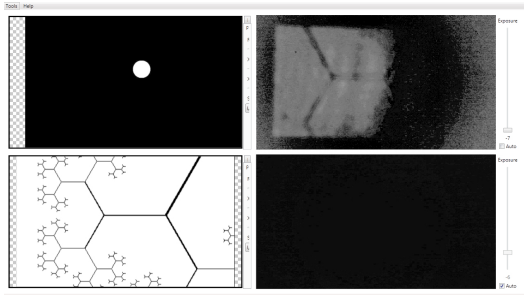

(d)

Figure 3.24: Reconstructed images of a fractal tree image written to the object mask being spatially filtered with a low pass filter of various sizes. The images were digitally enhanced to make the filtered image more visible.

CHAPTER 4

USING THE APPARATUS

This chapter will describe some of the demonstrations that can be created with the experiment, how to finely align the filter mask, and some basic troubleshooting. A more detailed document containing the use of the apparatus can be found on-line [13].

4.1 General Start Up Procedure

(1) Ensure the laser light is illuminating LCD_1. If not, ensure proper alignment between the laser and the single mode fiber.

(2) Ensure the computer is booted up and the FOPSC software is running.

(3) Ensure the webcams are connected to the computer.

(4) Ensure the projectors are connected to the computer.

(5) Ensure the image of LCD_1 is visible on $CMOS_1$. If it is not visible, adjust $CMOS_1$ until it is visible.

(6) Power on the projectors. The "Power" button is labeled on the extracted control panel for each projector.

(7) Ensure the computer is set to "extend" the desktop. This will allow the software to write entire images to the LCD panels.

(8) Write images to both panels.

4.2 In Class Demonstrations

View the diffraction pattern of images displayed on LCD_1. Some examples are listed below. This is not an exhaustive list, as any image file can be written to LCD_1.

Single Slit - Files "Filters.05.jpg" and "Filters.07.jpg" in the "Filters" menus can be used to write single slit images to the object mask. The image controls can be used to vary the size and rotation of the slit. As the slit widens, notice the spacing of the dark fringes decreasing. As the slit is rotated, notice the diffraction patterns rotating as well.

Double Slit - Any image of a double slit feature can be written to LCD_1. The image controls can be used to vary the size of the image as well as the rotation. Notice the effects on the spacing of the dark fringes, as well as the envelope of the single slit diffraction pattern as both the width of the slits and their spacing changes.

Circles - Files "Filters.01.jpg," "Filters.02.jpg," "Filters.03.jpg," and "Filters.04.jpg" in the "Filters" menu can be used to write circles to the object mask. Notice the effects of enlarging an image of a small circle ("Filters.01.jpg" and "Filters.02.jpg"). The pixelation of the circle causes non-circular features to be present. Notice what happens when the image is rotated. Use an image of a large circle ("Filters.03.jpg" and "Filters.04.jpg") to see the circular Airy diffraction pattern. Notice what happens when the size of this image change. The spacing of the rings in the diffraction pattern is inversely proportional to the size of the circle.

Spatially filter images displayed on LCD_1 with filters displayed on LCD_2.

Below are general suggestions. This is not an exhaustive list, as any image file can be written to LCD_1 and LCD_2.

- Vertical or Horizontal lines - Various images in the "Images" menu can be used which contain vertical and horizontal lines. The files "Filters.05.jpg," "Filters.06.jpg," "Filters.07.jpg," "Filters.08.jpg" available in the "Filters" menu can be used as the filters. Horizontal features in the object mask are filtered with vertical bars, and vertical features in the object mask are filtered with horizontal bars.

  Fractals - A low pass filter, files "Filters.01.jpg," "Filters.02.jpg," "Filters.03.jpg," and "Filters.04.jpg" available in the "Filters" menu can be used to filter fine details from fractals. High pass filters, files "Filters.09.jpg," "Filters.10.jpg," "Filters.11.jpg," and "Filters.12.jpg" can also be used for filtering fractals.

It is best when creating both objects and filters to use high contrast pictures with broad lines. Any feature with spacing less than 5 pixels will be blocked by LCD_2 (see Equation 3.3). The image controls in the software allow the contrast, size, rotation, and alignment on the screen to be adjusted.

4.3 Aligning the Components

To align the filter mask, use vertical lines as the object, then place a horizontal line filter on the filter mask. Ensure the filter is centered on the screen and reduce the size. Manually align the filter screen using the micrometers attached to the filter mask to maximize the filtering (the vertical lines will disappear). Do the same using horizontal lines as the object and a vertical line filter for the filter.

The final CMOS detector which images the filtered object mask is mounted on a translational stage which can be easily adjusted to create the sharpest image.

4.4 Troubleshooting

The illumination should be visible on LCD_1. If it is not, ensure the single mode fiber is properly aligned with the laser and adjusted for maximum output.

The image of LCD_1 should be visible on $CMOS_1$. If it is not, ensure proper alignment of equipment (beginning with $CMOS_1$) then ensure proper calibration of polarizers (the first two polarizers should be set to 0° and the last polarizer set to 65°).

If the projector is not responding, check all cord connections, then press the "source" button while computer is on and connected. The "source" button is labeled on the extracted control panel for each projector. If it is still not responding, try rebooting the computer.

An Asus brand laptop with Windows 7 Service Pack 1 64-bit operating system with an Intel Core i7-3610 QM 2.30 GHz CPU and an Nvidia GeForce GT 650M video card was used with the software and found to be unreliable. The images were not being written to the LCD panels as they were appearing in the red and blue channel windows. An Apple MacBook Pro with a Bootcamp Windows 7 Service Pack 1 operating system boot sector was used without fault. The MacBook has an Intel Core i5 processor, an Intel HD Graphics 4000 video card.

· BIBLIOGRAPHY

[1] Goodman, Joseph W. *Introduction to Fourier Optics*. Greenwood Village, CO: Roberts & Company Publishers, 2005

[2] Born, Max and Wolf, Emily. *Principles of Optics*. Cambridge, United Kingdom: Cambridge University Press, 2003

[3] Pedrotti, Frank L. S.J. and Pedrotti, Leno S. *Introduction to Optics*. Upper Saddle River, New Jersey: Prentice-Hall, Inc., 1993

[4] Wikipedia. *Rayleigh length*. `http://en.wikipedia.org/w/index.php?title=Rayleigh_length&oldid=568162769`. Web. 09 Mar. 2014.

[5] Halliday, David, Resnick, Robert, Walker, Jearl. *Fundamentals of Physics*. New York, New York: John Wiley & Sons, Inc.

[6] Weisstein, Eric W. *Nyquist Frequency*. From MathWorld–A Wolfram Web Resource. `http://mathworld.wolfram.com/NyquistFrequency.html`. Web. 10 Mar. 2014.

[7] Wikipedia. *Fractal*. Wikipedia, The Free Encyclopedia. 2014. `http://en.wikipedia.org/w/ index.php?title=Fractal&oldid=597893547`. Web. 09 Mar. 2014.

[8] Wikipedia. *Koch snowflake*. `http://en.wikipedia.org/w/index.php?title=Koch_snowflake&oldid=597956557`. Web. 09 Mar. 2014.

[9] Wikipedia contributors. *Laser safety*. Wikipedia, The Free Encyclopedia. `http://en.wikipedia.org/w/index.php?title=Laser_safety&oldid=598526476`. Web. 20 Mar. 2014.

[10] Saleh, B.E.A. and Teich, *M.C. Fundamentals of Photonics*. Hoboken, New Jersey: John Wiley & Sons, Inc.

[11] Fisher, Troy. *Fourier Optics Project Software*. `https://sjsuphys220e.pbworks.com/w/page/42365093/Fourier%20Optics%20Project%20Software`. Web. 10 Mar. 2014.

[12] Beyersdorf, Peter. *Laser Camera*. `http://www.youtube.com/watch?v=mBwH2hqGkck`. Web. 10 Mar 2014.

[13] Wilson, Nicolle. *In-class Spatial Filtering Demonstration Apparatus User Guide*. https://sjsuphys220e.pbworks.com/w/file/77715566/In-class%20Spatial%20Filtering%20Demonstration\%20Apparatus%20User%20Guide.pdf. Web. 30 Mar. 2014.

APPENDIX A

MATHEMATICA CODE

The Mathematica code used for this project is presented below.

This is the code to simulate the effect of discretizing the image by displaying it on an LCD panel. For our apparatus the pixel size is approximately 8 μm with a pixel fill factor of 0.8.

```
PixelFunction[x_, y_, linearratio_, scalefactor_] :=
  Module[{value, result},
   value = 1;
   If[Mod[x, scalefactor] < scalefactor*linearratio, value = 1*value,
    value = 0*value];
   If[Mod[y, scalefactor] < scalefactor*linearratio, value = 1*value,
    value = 0*value];
   result = value
   ];
```

To perform a Fourier transform of an image for data calculation, the following code is used:

```
FFT[image_]:=Module[{date,col,row,f,four,result},
data=ImageData[image];
col=First[ImageDimension[image]];
row=Last[ImageDimension[image]];
```

```
f=Sqrt[data];
four=Fourier[f,FourierParameters->{0,-1}];
result=four
];
```

This code takes the inverse Fourier transform of the image data.

```
iFFT[data_]:=Module[{col,row,f,four,result}],
f=data;
four=InverseFourier[f,FourierParameters->{0,-1}];
result=four
];
```

The diffraction pattern seen is not the Fourier transform, but the Fourier transform squared, or the power spectral density. The following code calculates the the power spectral density (PSD) for a given image.

```
PSD[image_]:=Module[{data,col,row,f,four,result}],
data=ImageData[image];
col=First[ImageDimensions[image]];
row=Last[ImageDimensions[image]];
f=data;
four=Fourier[f,FourierParameters->,{0,-1}];
result=Image[Abs[RotateRight[four,[IntegerPart[row/2],IntegerPart[col/2]}]]^2]
];
```

In order to enhance features with smaller intensities, the images are displayed on a logarithm scale.

```
LogPSD[image_]:=Module[{data,col,row,f,four,result},
data = ImageData[image;
col = First[ImageDimensions[image]];
row = Last[ImageDimensions[image]];
f = data;
four = Fourier[f,FourierParameters->{0,-1}];
result = Image[
(1+Log[$MachineEpsilon+Abs[
RotateRight[four,{integerPart[row/2,IntegerPart[col/2]}]]^2]/10]
];
```

This function simulates the contrast, the amount of light which is let through the object and filter masks. In a design of the experiment which uses transparencies as the object and filter masks, the contrast is fairly low. This lets a certain amount of light through areas which we are trying to block in the filter mask. The filtering is not exact and the resulting diffraction pattern and reconstructed image are not what is calculated.

```
Contrast[M_,c_]:= M*c+(1-c)
```

In order to filter an object image with a filter image, the following code can be used. Notice the final image is the absolute value squared of the calculated values for the filtered image data.

```
Image[Abs[
   iFFT[Contrast[FilterFromImage[LPF[display, 40]], 0.9]*
     FFT[display]]]^2]
```

This code is used to import an image from an image file located on a computer.

```
SetDirectory["c:/fourier_images"];
img = Import["testimg.jpg"];
width = ImageDimensions[img][[1]];
height = ImageDimensions[img][[2]];
greyscaleimage = ColorSeparate[ColorConvert[img,"HSD"]][[3]];
filter = FilterFromImage[bigfilterimg];
```

This is a table loop to vary the parameters of a horizontal bar filter in order to see the effects of different parameters on the reconstructed image.

```
Do[Print[Table[
   Image[Abs[
      iFFT[FilterFromImage[
         ImageMultiply[HBarFilter[imagetable[[j]], 2, i], grid]]*
        FFT[imagetable[[j]]]]]^2], {i, 1, 8, 2}]], {j, 3}]
```

This code is used to convert an image of a filter into a form which can be used to filter an object image.

```
FilterFromImage[image_] :=
  Module[{data, col, row, px, f, four, result},
   data = ImageData[image];
   col = First[ImageDimensions[image]];
   row = Last[ImageDimensions[image]];
   px = col*row;
   result =
```

```
    Abs[RotateRight[data, {IntegerPart[row/2], IntegerPart[col/2]}]]^2
   ];
```

This code generates a high pass filter with a variable radius based on dimensions of a reference image.

```
HPF[image_, radius_] := Module[{data, col, row, result},
   col = First[ImageDimensions[image]];
   row = Last[ImageDimensions[image]];
   data =
    Table[If[(i - (col + 1)/2)^2 + (j - (row + 1)/2)^2 > radius^2, 1,
      0]  , {j, row}, {i, col}];
   result = Image[data]
   ];
```

This code generates a low pass filter with a variable radius based on dimensions of a reference image.

```
LPF[image_, radius_] := Module[{data, col, row, result},
   col = First[ImageDimensions[image]];
   row = Last[ImageDimensions[image]];
   data =
    Table[If[(i - (col + 1)/2)^2 + (j - (row + 1)/2)^2 > radius^2, 0,
      1]  , {j, row}, {i, col}];
   result = Image[data]
   ];
```

This code generates a horizontal bar filter with variable radius and thickness based on dimensions of a reference image.

```
HorizontalBarFilterImage[image_, radius_, thickness_] :=
  Module[{data, col, row, result},
   col = First[ImageDimensions[image]];
   row = Last[ImageDimensions[image]];
   t3 = Table[
     If[(i - (col + 1)/2)^2 + (j - (row + 1)/2)^2 < radius^2, 1,
      If[Abs[(j - (row + 1)/2)] < thickness, 0, 1]], {j, row}, {i,
      col}];
   result = Image[t3]
   ];
```

This code generates a vertical bar filter with variable radius and thickness based on dimensions of a reference image.

```
VerticalBarFilterImage[image_, radius_, thickness_] :=
  Module[{data, col, row, result},
   t2 = FFT[image];
   col = First[ImageDimensions[image]];
   row = Last[ImageDimensions[image]];
   t3 = Table[
     If[(i - (col + 1)/2)^2 + (j - (row + 1)/2)^2 < radius^2, 1,
      If[Abs[(i - (col + 1)/2)] < thickness, 0, 1]], {j, row}, {i,
      col}];
   result = Image[t3]
   ];
```

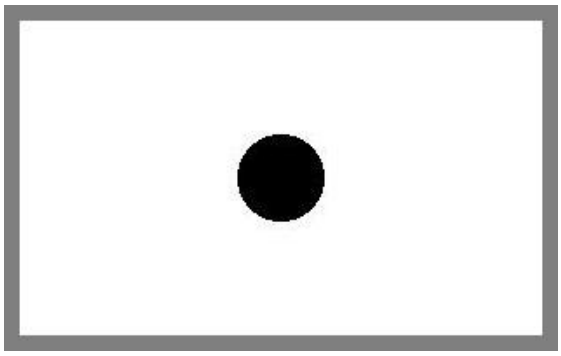

(a) High pass filter.

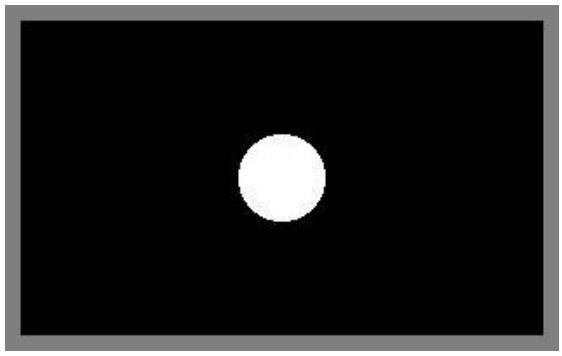

(b) Low pass filter.

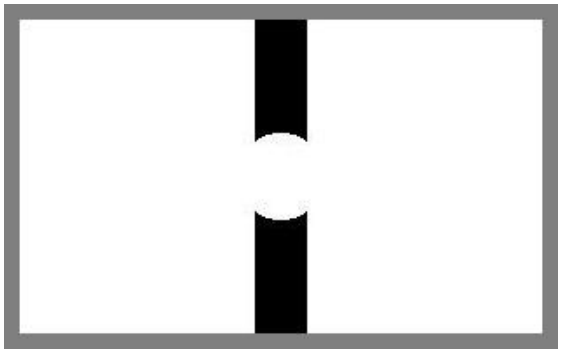

(c) Vertical bar filter. The center of the filter is left open to allow the structure of the rest of the image to pass through

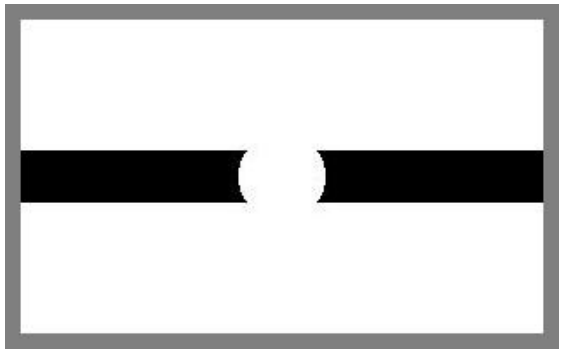

(d) Horizontal bar filter. The center of the filter is left open to allow the structure of the rest of the image to pass through

Figure A.1: Various filters generated with Mathematica.

APPENDIX B

PARTS LIST

Below is a list of all of the parts used in this experiment.

- Two Projectors
- Three Polarizers
- Two Webcams with the CMOS exposed
- One beam splitter
- Monochromatic light source
- Single mode fiber
- Optics table (or sturdy table)
- One windows computer with Fourier Optics System Control software installed [11]
- Two VGA Cables
- One VGA splitter
- One two-port USB hub

Below are the specific components used in this experiment

- (2) Epson PowerLite Home Cinema 705 HD 720p Home theater projectors
- (2) Webcams Logitech C525 webcams
- (1) Helium-neon laser
- (4) 2” diameter plano-convex N-BK7 anti-reflection coated glass lenses
- (1) Thorlabs 2 m single mode fiber suitable for light 600 nm - 800 nm with a numerical aperture of 0.12
- (1) Apple MacBook Pro dual boot with Windows 7 Service Pack 1 installed